Optical and Near-Infrared Observations of the Peculiar Type Ia Supernova 1999ac[1]

Mark M. Phillips,[2] Kevin Krisciunas,[3] Nicholas B. Suntzeff,[4] R. G. Abraham,[5] M. G. Beckett,[6] Marco Bonati,[4] Pablo Candia,[7] T. Michael Corwin,[8] Darren L. Depoy,[9] Juan Espinoza,[4] Andrew E. Firth,[10] Wendy L. Freedman,[5] Gaspar Galaz,[11] Lisa Germany,[12] David Gonzalez,[4] Mario Hamuy,[14] N. C. Hastings,[13] Aimee L. Hungerford,[15] Valentin D. Ivanov,[12] Erika Labbé,[11] Ronald O. Marzke,[6] Patrick J. McCarthy,[5] Richard G. McMahon,[10] Russet McMillan,[13] Cesar Muena,[2] S. E. Persson,[5] Miguel Roth,[2] María Teresa Ruiz,[14] R. Chris Smith,[4] Roger Smith,[16] Louis-Gregory Strolger,[17] and Christopher Stubbs[18]

ABSTRACT

[1]Based in part on observations taken at the Cerro Tololo Inter-American Observatory, National Optical Astronomy Observatory, which is operated by the Association of Universities for Research in Astronomy, Inc. (AURA) under cooperative agreement with the National Science Foundation. This paper is also based in part on observations obtained with the Apache Point Observatory 3.5-meter telescope, which is owned and operated by the Astrophysical Research Consortium.

[2]Las Campanas Observatory, Carnegie Observatories, Casilla 601, La Serena, Chile; mmp@lco.cl, miguel@lco.cl

[3]University of Notre Dame, Department of Physics, 225 Nieuwland Science Hall, Notre Dame, IN 46556-5670; kkrisciu@nd.edu

[4]Cerro Tololo Inter-American Observatory, Casilla 603, La Serena, Chile; nsuntzeff@noao.edu, jespinoza@ctio.noao.edu, dgonzalez@ctio.noao.edu, csmith@ctio.noao.edu

[5]Observatories of the Carnegie Institution of Washington, 813 Santa Barbara Street, Pasadena, CA 91101; wendy@ociw.edu, pmc2@ociw.edu, persson@ociw.edu

[6]San Franciso State University, Physics and Astronomy, 1600 Holloway Avenue, San Francisco, CA 94132-4163; marzke@stars.sfsu.edu

[7]Gemini Operations Center, Casilla 603, La Serena, Chile; pcandia@gemini.edu

[8]University of North Carolina at Charlotte, Department of Physics, Charlotte, NC 28223; mcorwin@uncc.edu

[9]Ohio State University, Department of Astronomy, 140 W. 18th Avenue, Columbus, OH 43210; depoy@astronomy.ohio-state.edu

[10]Institute of Astronomy, Madingley Road, Cambridge, CB3 0HA, England, UK; rgm@ast.cam.ac.uk

[11]Departamento de Astronomía y Astrofisica, Pontificia Universidad Catolica de Chile, Casilla 306, Santiago 22, Chile; ggalaz@astro.puc.cl, elabbe@astro.puc.cl

[12]European Southern Observatory, Avenida Alonso de Cordova 3107, Vitacura, Casilla 19001, Santiago 19, Chile; lgermany@eso.org, vivanov@eso.org

[13]Apache Point Observatory, P. O. Box 59, Sunspot, NM 88349-0059; hastings@apo.nmsu.edu, rmcmillan@apo.nmsu.edu

[14]Universidad de Chile, Departmento de Astronomía, Casilla 36-D, Santiago, Chile; mhamuy@das.uchile.cl, mtruiz@das.uchile.cl

[15]CCS-4, MS D409, Los Alamos National Laboratory, Los Alamos, NM 87545; aimee@lanl.gov

[16]California Institute of Technology, Astronomy Department, MS 105-24, Pasadena, CA 91125; rsmith@astro.caltech.edu

[17]Department of Physics and Astronomy, Western Kentucky University, 1906 College Heights Blvd. #11077, Bowling Green, KY 42101-1077; louis.strolger@wku.edu

[18]Department of Physics and Department of Astronomy, 17 Oxford Street, Harvard University, Cambridge

We present 39 nights of optical photometry, 34 nights of infrared photometry, and 4 nights of optical spectroscopy of the Type Ia SN 1999ac. This supernova was discovered two weeks before maximum light, and observations were begun shortly thereafter. At early times its spectra resembled the unusual SN 1999aa and were characterized by very high velocities in the Ca II H&K lines, but very low velocities in the Si II λ 6355 line. The optical photometry showed a slow rise to peak brightness but, quite peculiarly, was followed by a more rapid decline from maximum. Thus, the B- and V-band light curves cannot be characterized by a single stretch factor. We argue that the best measure of the nature of this object is *not* the decline rate parameter $\Delta m_{15}(B)$. The $B-V$ colors were unusual from 30 to 90 days after maximum light in that they evolved to bluer values at a much slower rate than normal Type Ia supernovae. The spectra and bolometric light curve indicate that this event was similar to the spectroscopically peculiar slow decliner SN 1999aa.

Subject headings: supernovae: individual (SN 1999ac) — supernovae: photometry — supernovae: spectroscopy

1. Introduction

Due to their considerable potential as extragalactic standard candles, Type Ia supernovae (SNe Ia) have been the subject of intense study during the last 15 years. Although it has by now been amply demonstrated that SNe Ia cover a range in instrinsic brightness of a factor of two or more (see Leibundgut 2000, and references therein), the fortuitous existence of a correlation between the peak luminosity and the rate of decline from maximum of the B light curve, including prescriptions for color corrections (Phillips 1993; Hamuy et al. 1996b; Riess, Press & Kirshner 1996; Phillips et al. 1999; Nobili et al. 2003; Guy et al. 2005), has allowed distances to be measured to better than 10 percent to redshifts $z \leq 0.1$ (Hamuy et al. 1996a; Riess, Press & Kirshner 1996). Because they can be observed to very large distances, SNe Ia have become the tool of choice for measuring the Hubble constant (e.g., Hamuy et al. 1996a; Riess, Press & Kirshner 1996; Sandage et al. 1996; Jha et al. 1999; Suntzeff et al. 1999; Phillips et al. 1999; Tripp & Branch 1999; Gibson et al. 2000; Parodi et al. 2000; Freedman et al. 2001; Phillips et al. 2003; Riess et al. 2005) and, in combination with measurements of fluctuations in the microwave background radiation (Bennett et al. 2003), have provided compelling evidence for an accelerating universe (Garnavich et al. 1998;

MA 02138; cstubbs@fas.harvard.edu

Riess et al. 1998; Perlmutter et al. 1999; Tonry et al. 2003; Knop et al. 2003; Barris et al. 2004; Riess et al. 2004; Krisciunas et al. 2005).

Although the majority of SNe Ia display very similar spectral evolution, roughly one-third of all events show spectroscopic peculiarities (Li et al. 2001a). Three well-observed examples – SN 1991T, SN 1991bg, and SN 1986G – have served as the prototypes of spectroscopically-peculiar SNe Ia (Branch, Fisher, & Nugent 1993).

The pre-maximum optical spectra of SN 1991T showed unusually weak lines of Si II, S II, and Ca II, while at the same time displaying prominent high-excitation features of Fe III (Filippenko et al. 1992a; Phillips et al. 1992). The Si II, S II, and Ca II lines grew quickly in strength following maximum until the spectrum appeared essentially normal a few weeks past maximum. SN 1991T dimmed slowly from maximum and was originally thought to be considerably more luminous than "normal" SNe Ia (Filippenko et al. 1992a; Phillips et al. 1992), although the Cepheid distance to the host galaxy, NGC 4527, obtained later with the Hubble Space Telescope, implies that this supernova was only moderately over-luminous (Saha et al. 2001; Gibson & Stetson 2001).

The main spectroscopic peculiarity of SN 1991bg was the presence at maximum light of a broad absorption trough at 4100-4400 Å due mostly to Ti II lines (Filippenko et al. 1992b; Leibundgut et al. 1993; Turatto et al. 1996; Mazzali et al. 1997), reflecting a lower effective temperature. As a consequence, SN 1991bg was unusually red ($B - V \simeq 0.75$) at maximum light. SN 1986G was similar to 1991bg, but less extreme (Phillips et al. 1987; Cristiani et al. 1992). Both events were substantially sub-luminous.

Nugent et al. (1995) have shown that the photometric sequence of SNe Ia (i.e., the luminosity vs. decline rate relation) also manifests itself as a spectroscopic sequence which can be modelled in terms of a range in the effective temperature at maximum. The luminous, slowly-declining SN 1991T represents the high-temperature extreme of the sequence, while the fast-declining, sub-luminous SN 1986G and SN 1991bg correspond to the low-temperature limit. Under this scenario, none of these three SNe Ia should be considered "peculiar". However, not all luminous, slow-declining SNe Ia display SN 1991T-like pre-maximum spectra – e.g., SN 1992bc (Maza et al. 1994) and SN 1999ee (Hamuy et al. 2002) – so it is not clear if this interpretation is fully correct. Moreover, the last few years have revealed the existence of several SNe Ia which are of an intermediate type between SN 1991T events and "normal" SNe Ia. The prototype of these objects, which may be more common than SN 1991T-like events, is SN 1999aa (Krisciunas et al. 2000; Li et al. 2001a; Garavini et al. 2004). SN 1999aa was similar to SN 1991T in displaying very weak Si II 6150 Å absorption and prominent Fe III lines in its pre-maximum spectra, but it showed strong Ca II H & K absorption at the same epoch in which this feature was weak or absent in SN 1991T (Filip-

penko, Li, & Leonard 1999). By maximum light the spectrum of SN 1999aa had evolved to that of a "normal" Type Ia supernova. Hence, SN 1999aa-like events would be difficult, if not impossible, to distinguish spectroscopically unless a spectrum were obtained at least a week before maximum.

In order to more fully understand the range of spectroscopic and photometric characteristics of SNe Ia, we have organized a number of observing campaigns to obtain optical photometry, infrared photometry, and optical spectroscopy of nearby events ($z \leq 0.05$). In this paper, we present observations obtained of the SN 1999aa-like object SN 1999ac. SN 1999ac was discovered in the Sc galaxy NGC 6063 by Modjaz et al. (1999) from images obtained on 1999 February 26.5 and 27.5 UT. It was located at RA = 16:07:15.0, DEC = +07:58:20 (equinox 2000), some 24 arcsec east and 30 arcsec south of the core of its host. SN 1999ac was confirmed to be a Type Ia supernova by Phillips & Kunkel (1999) from a spectrum taken on February 28 UT, who also noted that the spectrum was similar to that of the slow decliner SN 1991T (Lira et al. 1998). Like SN 1991T, the Fe III lines at 4300 and 5000 Å in the spectrum of SN 1999ac were observed to be strong and the Si II 6355 Å absorption weak; but unlike 1991T, the Ca II H & K absorption in SN 1999ac was strong and well-developed. Phillips & Kunkel speculated that SN 1999ac had been caught near, or a few days before, maximum; our observations show that B maximum did not actually occur until 13 days after this first spectrum was obtained.

In §2 we present our optical and near-infrared photometry of SN 1999ac. The resulting light curves, which are among the most complete ever obtained of a SN Ia for the first few months following explosion, are contrasted with the light curves of other well-observed SNe Ia. In §3 we discuss the optical spectra obtained, likewise comparing these with similar observations of both spectroscopically "normal" and "peculiar" SNe Ia. In §4 we derive the most likely host galaxy reddening for SN 1999ac, and compare the peak luminosity and bolometric light curve with those of more typical SNe Ia. Finally, in §5 the conclusions of this investigation are summarized.

2. Optical and Infrared Photometry

2.1. Observations and Data Reduction

Optical $BV(RI)_{KC}$ imaging of SN 1999ac commenced at the Cerro Tololo Inter-American Observatory (CTIO) on 1999 March 1 UT, and observations were continued for nearly five

months.[19] Three different telescopes – the 0.9 m, 1.5 m, and the Yale-AURA-Lisbon-Ohio (YALO) 1.0 m – were employed. In addition, three nights of optical imaging were obtained with the Apache Point Obervatory (APO) 3.5 m telescope.

In Fig. 1 we show an optical finding chart of the field. A sequence of local "standards" in the supernova field was established from observations obtained on multiple photometric nights. The $BV(RI)_{KC}$ magnitudes for these stars are given in Table 1 and are tied to observations of Landolt (1992) standards obtained on the same nights. We reduced the optical data for SN 1999ac with respect to the local standards using color coefficients derived from the observations of the Landolt stars. The local standards were verified to be constant over the $\sim$5 month duration of our observation. This method of data reduction allows one to observe the SN even under non-photometric conditions, under the explicit assumption that terrestrial clouds are grey (i.e. do not selectively filter out light of one color more than another). In our experience this is demonstrably valid as long as the exposures are not extremely short, or the clouds extremely thick. For more on the greyness of terrestrial clouds see Serkowski (1970), Walker et al. (1971), and Olsen (1983).

We present $BV(RI)_{KC}$ photometry of SN 1999ac in Table 2. All magnitudes were determined with DAOPHOT (Stetson 1987, 1990) using PSF (point spread function) photometry on direct, non-subtracted images. The brightness and location of the SN did not require the use of host galaxy subtraction templates.

Near-infrared imaging of SN 1999ac in the J_sHK_s bands was obtained over a three month period beginning on the night of 1999 February 28 UT. Most of the data were obtained at the Las Campanas Observatory (LCO) with the Swope 1.0 m and du Pont 2.5 m telescopes. A few images in H and K_s were also obtained with the Steward Observatory (SO) 2.3 m and 1.5 m telescopes. In a similar manner to the optical photometry, a sequence of local standards was established from observations made with the LCO 1.0 m telescope on photometric nights. In Table 3 we give the near infrared magnitudes for the seven field stars, which are tied to the infrared standards of Persson et al. (1998). Two of these stars (IR3 and IR7) were very red and were too faint in the optical bands to be useful as optical standards, but IR3 was the principal star used to reduce the infrared photometry. From a comparison of the differential magnitudes of IR3 with respect to field stars 1 and 8, we established that IR3 was constant at the 0.03 mag level during the period of our observations.

The final J_sHK_s magnitudes of SN 1999ac are given in Table 4. These were derived using the same PSF photometry software employed for the optical data. Since most of the IR

[19]Our R- and I-band data were obtained with "Kron-Cousins" filters (Bessell 1979). For the sake of simplicity we shall drop the KC subscripts when referring to RI data.

imaging was obtained with the LCO 1.0 m telescope and infrared camera, which is the very telescope and instrument used to establish the system of standards of Persson et al. (1998), no color corrections were applied to the IR photometry. We also note that the system of Persson et al. (1998) uses different filters than the standard J-band and K-band filters. The J_s and K_s filters (where "s" stands for "short") have slightly different effective wavelengths and narrower bandwidths than the corresponding Johnson filters.

2.2. Optical Photometry

The $BVRI$ light curves of SN 1999ac are shown in Fig. 2. The symbols identify the data taken with the different telescopes employed. Also included are the published observations of Jha (2002).

It may be seen that our optical photometry began ∼12 days before B maximum was reached, providing an uninterrupted record of the rise to peak brightness in each band and continuing without significant gaps to ∼4 months after B maximum. Except for the YALO 1.0 m observations, the data obtained with the various telescopes, including the published measurements of Jha (2002), are in generally good agreement. The YALO 1.0 m photometry shows significant discrepancies, most notably in the R band, but also clearly present in B, V, and I, particularly near maximum light. These differences are accentuated in Fig. 3 which shows the evolution of the $B-V$, $V-R$, and $V-I$ colors. Note that the early $B-V$ points from the YALO 1.0 m are nearly 0.2 mag redder than the trend defined by the 0.9 m and Jha (2002) photometry, but that this difference has essentially disappeared by JD 2,451,295. In $V-R$ the differences are even larger and persist during the entire period that the YALO 1.0 m was utilized. In $V-I$ the agreement is the best, but this is fortuitous since the YALO 1.0 m V and I points are both clearly "too bright" at early epochs (see Fig. 2). Similar problems with data obtained for other SNe Ia with the YALO 1.0 m R filter have been documented (see Suntzeff 2000; Stritzinger et al. 2002); indeed, this filter was replaced in 2001 by a filter which provides a much better match to the Kron-Cousins system. Problems with SN Ia photometry taken with the YALO B and V filters have also been observed by Krisciunas et al. (2003) and Candia et al. (2003). In principle, with precise knowledge of the effective bandpasses of the different telescope/filter/CCD combinations and optical spectrophotometry with sufficient temporal coverage, it should be possible to correct all of the photometry, including the YALO observations, to the standard $BVRI$ system as defined by Bessell (1990). To date, however, attempts to do this have been only partially successful (Stritzinger et al. 2002; Krisciunas et al. 2003, 2004c). Since the YALO data are not needed to plug any critical gaps in the light curves, we can limit ourselves to a consideration of the

optical photometry based on the CTIO 0.9 m and 1.5 m telescopes.

The maximum light magnitudes in $BVRI$ and the Julian Dates that these were attained are listed in Table 5. Direct measurement of the B-band light curve of SN 1999ac yields a value of 1.32 ± 0.08 for the decline rate parameter $\Delta m_{15}(B)$, which is defined as the amount in magnitudes that the B light curve declines during the first 15 days following maximum (Phillips 1993). Correcting for a total (Galactic + host galaxy) reddening of $E(B-V) = 0.14$ (see §4.1), this value becomes $\Delta m_{15}(B) = 1.33$ (see Phillips et al. 1999) – but as we shall see, this value of the decline rate does not tell the whole truth about the light curves. As shown in Fig. 4, the shapes of the $BVRI$ light curves are complicated, and not really a good match to the light curves of other well-observed SNe Ia. Here the various light curve templates have all been adjusted to coincide at maximum light. Note, in particular, the poor correspondence with the light curves of SN 1994D, whose $\Delta m_{15}(B)$ value (1.32) matches that of SN 1999ac. Only over the first 15 days after maximum do the B-band light curves of these two SNe evolve in a similar fashion; at both earlier and later epochs the light curve of SN 1994D falls below that of SN 1999ac as if SN 1999ac were a slower riser and slower decliner than SN 1994D. The same is true in the V, R, and I bands.

In spite of these indications that SN 1999ac is a slower-declining event than the $\Delta m_{15}(B)$ measurement suggests, the comparisons with the slower declining SNe Ia in Fig. 4 are not without problems as well. Before maximum, SN 1999ac rose only slightly more quickly than SN 1991T. The V-band light curve of SN 1992al ($\Delta m_{15}(B) = 1.11$) is a reasonable match to the observations of 1999ac. However, data of SN 1992al in other passbands (specifically B, R, and I) poorly match SN 1999ac in the same passbands.

Note that in I, the secondary maximum occurs significantly earlier in SN 1994D than in SN 1999ac, which again indicates that SN 1999ac was effectively a slower decliner than SN 1994D (Hamuy et al. 1996b). However, the *strength* of the secondary maximum is more consistent with a faster-declining SN Ia. Following the recipe given by Krisciunas et al. (2001), we calculate a flux (with respect to maximum) of the secondary maximum between 20-40 days after B maximum of $\langle \mathrm{I} \rangle_{20-40} = 0.475$, which is good agreement with the expected value for a SN with $\Delta m_{15}(\mathrm{B}) = 1.33$.

The optical color evolution of SN 1999ac was similarly unique, as shown in Fig. 5. Here the data for SN 1999ac have been corrected for a Galactic reddening of $E(B-V) = 0.046$ (Schlegel, Finkbeiner & Davis 1998). The template curves with which the observations are compared have been corrected for both Galactic and host components of reddening as per Table 2 of Phillips et al. (1999). Included also for comparison is the photometry of SN 1999aa from Krisciunas et al. (2000) corrected for Galactic reddening only. Prior to the epoch of B maximum, the $B-V$ color of SN 1999ac did not differ significantly from those

of the other SNe Ia plotted. However, ∼5 days after maximum, SN 1999ac began to rapidly grow redder than all of the other SNe, reaching a maximum difference in $B-V$ of several tenths of a magnitude by 10-15 days past maximum. By ∼30 days after maximum, however, the $B-V$ color of SN 1999ac once again resembled that of several of the comparison SNe, and continued to evolve in a similar fashion until around day 50, when the $B-V$ color of SN 1999ac once again began to slowly grow steadily redder than that of the other SNe. The peculiarities in the evolution of the $V-R$ photometry of SN 1999ac are nominally similar to those observed for $B-V$, with 1999ac starting off reasonably similar to the other events, growing significantly redder between 5-25 days after maximum, and then evolving back to a very similar color evolution by day 30. Except for the very first measurements obtained, the $V-I$ evolution of SN 1999ac was redder than that of the reference SNe during nearly the entire period covered by our observations. We call special attention to the fact that the optical color evolution of SN 1999ac was not at all like that of SN 1999aa. In spite of its spectroscopic peculiarities, the evolution of the latter SN was much more consistent with that of the template curves shown, particularly those corresponding to the slower decline rates.

2.3. Near-Infrared Photometry

The J_s, H, and K_s light curves of SN 1999ac are displayed in Fig. 6. As in the case of the optical light curves, the data obtained with the various telescopes have been plotted with different symbols. These observations provide excellent coverage of the rise to maximum light in the near-infrared. In the J_s band, this rise is followed by a nearly symmetric decline which levels off at ∼15 days after maximum was reached. Unfortunately, a 14-day gap in the observations then occurs, after which the light curve is observed to decline again. The impression is that, much like the I-band light curve, the secondary maximum in J_s was actually more of a "plateau" rather than a clearly-defined peak.

The maximum light magnitudes in J_sHK_s and the corresponding Julian Dates are listed in Table 5. As with other well-observed SNe Ia, the J_sHK_s maxima all occurred ∼2-3 days before B-band maximum. In H and K_s, the initial rise to maximum is similar to that observed in J_s. This is followed in both bands by only a slight decrease in magnitude, to a plateau ∼10-15 days after maximum. Then there is a 20-day gap when only a single H-band observation was obtained. By 35-40 days past the initial maximum, both the H- and K_s-band light curves began a decline phase which was probably initially somewhat more rapid than at later times (see particularly the K_s-band observations).

Fig. 6 also includes near-infrared photometric loci for three spectroscopically normal

objects: SN 1998bu (Jha et al. 1999; Hernandez et al. 2000), SN 1999ee (Krisciunas et al. 2004b), and SN 2001el (Krisciunas et al. 2003). The decline rates of these three SNe are $\Delta m_{15}(B) = 1.01 \pm 0.05$, 0.94 ± 0.06, and 1.13 ± 0.04, respectively. SN 1999ee was a slow decliner, but did *not* exhibit the doubly ionized lines characteristic of SN 1991T-like objects (Hamuy et al. 2002). SNe 1998bu and 2001el were normal mid-range decliners. Fig. 6 shows that the near-IR light curves of SNe 1999ac and 2001el match reasonably well in the first 20 days after the IR maxima. SN 1999ac was fainter at 10 days before and 40 days after $T(B_{max})$, consistent with its larger value of $\Delta m_{15}(B)$.

While there are still very few SN Ia that have well sampled near-IR light curves, certain trends are suggested by the presently available data. Objects with small values of $\Delta m_{15}(B)$ are also slower risers/decliners in the IR. Objects with larger values of $\Delta m_{15}(B)$ are faster risers/decliners in the IR. In the I-band the slow decliners have later secondary peaks (Hamuy et al. 1996b; Riess, Press & Kirshner 1996; Nobili et al. 2005). This trend seems to hold for the near-IR as well.

In Fig. 7 we show the $BVIJ_sHK_s$ data of SN 1999ac within ± 20 days of B maximum along with various single-band templates. The time-since-maximum-light has been scaled according to stretch factors derived from $\Delta m_{15}(B)$(Jha 2002, Fig. 3.8). Time dilation is also taken into account. If $\Delta m_{15}(B)$ is a representative measure of the light curve characteristics, the stretched data should lie on top of the templates. This is clearly not the case. At early times the BVI data are several tenths of a magnitude "too bright". The J_s data conform to the template at early times, but the I and J_s data are too bright after $T(B_{max})$. Only in the K_s band do the data conform closely to the template before and after maximum light.

The $V - J_s$, $V - H$, and $V - K_s$ color evolution of SN 1999ac is shown in Fig. 8. We have also added the V *minus* near-IR color loci from Krisciunas et al. (2000) offset by various amounts (see §4.1). Because the early time V-band data are brighter than we would expect on the basis of $\Delta m_{15}(B)$ alone, the V *minus* near-IR colors are much too blue at early times. Since the V and K_s data conform to the templates from 0 to 20 d after $T(B_{max})$, the most reliable color index for the purposes of determining a color excess and extinction may well be $V - K_s$ at this epoch.

3. Optical Spectroscopy

Four optical spectra of SN 1999ac covering phases from 13 days before to 41 days after B maximum were obtained with the LCO 2.5 m du Pont telescope and WFCCD spectrograph. The specific dates and phases, as well as the wavelength coverage and resolution of these

spectra, are given in Table 6. The spectra are plotted in Fig. 9. Note that the last spectrum of 23 April (UT) was acquired under poor transparency conditions and consequently suffers from low signal-to-noise. The version of this spectrum shown in Fig. 9 has therefore been smoothed to an effective resolution of 90 Å.

The strongest features in the spectrum of SN 1999ac obtained at −13 days are identified with Ca II, Fe III, and Si II. This spectrum is compared in Fig. 10 with comparable-phase spectra of SN 1991T, SN 1999aa, and SN 1990N. The overall impression is that these four SNe form an orderly sequence, with the peculiar SN 1991T at the one extreme and the "normal" SN 1990N at the other. Note, in particular, how the strengths of the Ca II H&K and Si II λ6355 lines vary continuously from SN 1991T, where they are completely absent, to SN 1990N where they are the strongest features in the spectrum. This situation lends credence to the idea that SNe Ia like SN 1999aa and SN 1999ac are transition events (Li et al. 2001a; Branch 2001; Garavini et al. 2004). Spectra obtained around T(B_{max}) of these same four SNe strengthen this impression, as illustrated in Fig. 11. Once again, the strengths of the Ca II H&K and Si II λ6355 form a smooth sequence, with SN 1999ac lying intermediate between SN 1999aa and SN 1990N. By this phase, the S II $\lambda\lambda$5454,5460 lines have appeared in both SN 1999aa and SN 1999ac, making the peculiar nature of these events far less obvious than at earlier epochs. Indeed, Li et al. (2001a) have emphasized the difficulty of identifying SN 1999aa-like events in the absence of spectral observations obtained well before maximum light. Fig. 12 shows that by a week after B-band maximum, it is virtually impossible to discriminate spectroscopically between SN 1999ac and the "normal" SN 1990N.

Garavini et al. (2005) have recently presented a detailed analysis of the optical spectral evolution of SN 1999ac. Their data cover essentially the same time period (−15 to +42 days with respect to B maximum) as ours, but with more frequent temporal sampling. Their main conclusions are similar to those presented in the previous paragraph – i.e., that prior to maximum light, the spectra of SN 1999ac resembled those of SN 1999aa, but with stronger Ca II and Si II absorption, whereas after maximum the spectra appeared essentially normal. The Ca II H&K lines were found to exhibit larger than average expansion velocities from maximum light onward, whereas the iron lines appeared to be characterized by somewhat lower than average velocities. The Si II λ6355 expansion velocities decreased monotonically from −14 to +32 days, and are amongst the slowest ever observed. Expansion velocities measured from the minima of the Ca II H&K and Si II λ6355 lines in our spectra are given in the last two columns of Table 6. These are in good agreement with the measurements of Garavini et al. (2005). Our expansion velocity for Ca II H&K obtained at −13 days suggests that at epochs before maximum the calcium velocities were *not* unusually high, although very few SNe Ia have been observed at such early epochs.

Garavini et al. (2005) measured values for SN 1999ac of the $\mathcal{R}$(Si II), v_{10}(Si II), and $\dot{v}$ parameters [20] that, in combination with $\Delta m_{15}(B)$, Benetti et al. (2005) recently used to identify three subgroups of SNe Ia. In all three of the diagrams considered by Benetti et al. — $\Delta m_{15}(B)$ vs. $\mathcal{R}$(Si II), $\Delta m_{15}(B)$ vs. v_{10}(Si II), and $\Delta m_{15}(B)$ vs. $\dot{v}$ — SN 1999ac appears to be either an outlier or an extreme example of "normal" SNe Ia. Garavini et al. (2005) pointed out that the low value of $\mathcal{R}$(Si II) = 0.098±0.030 measured for SN 1999ac is consistent with high temperature (as manifested by the presence of strong Fe III absorption lines at early epochs), but is inconsistent with the value of $\Delta m_{15}(B)$= 1.33, suggesting that for this object $\Delta m_{15}(B)$ might not be a good indicator of luminosity. We will return to this point in §4.2.

4. Discussion

4.1. Host Galaxy Reddening

The location of SN 1999ac in the outer regions of its host galaxy and the lack of strong Na I D lines in the spectra (which would imply the existence of dust along the line of sight) lead us to believe that the host galaxy reddening of this SN should be small. Estimating the host galaxy reddening of SN 1999ac is not so straight forward due to the peculiarities in the evolution of the various observed colors. If we follow the procedures detailed in Phillips et al. (1999) using the measured value of the decline rate $\Delta m_{15}(B) = 1.32 \pm 0.08$, the BVI data imply a host galaxy reddening of E(B−V) = 0.12 ± 0.03 mag. If the dust along the line of sight can be characterized as having a ratio of total to selective absorption $R_V \equiv A_V/E(B-V) = 3.1$ (Sneden et al. 1978), then A_V(host) = 0.37 ± 0.09 mag and A_V(tot) = 0.51 ± 0.09 mag. However, it should be noted that one of the pillars of the Phillips et al. method is the assumption that all SNe Ia follow essentially the same $B - V$ evolution at late times (30-90 days after V-band maximum). Fig. 5 shows that this is not the case for SN 1999ac in that the data from 30 to 90 days after V maximum are best fitted by a slope of -0.0073 ± 0.0004 mag d^{-1}, which is clearly shallower than the value of -0.0118 mag d^{-1} given by Lira (1995).[21]

[20] $\mathcal{R}$(Si II) is the ratio of the depth of Si II 5800 Å to Si II 6100 Å absorption. It is theorized to be driven by temperature, hence the ^{56}Ni mass synthesized in the explosion. v_{10}(Si II) is the blueshift measured in the Si II λ6355 line ten days after maximum light. $\dot{v}$ is an estimate of the expansion velocity time derivative computed after maximum light.

[21] Two other SN Ia whose color evolution did not allow the unambiguous determination of color excesses were the highly peculiar SN 2000cx (Li et al. 2001b; Candia et al. 2003) and SN 2002bo (Benetti et al. 2004;

If we maximize the wavelength difference of two "well behaved" photometric bands, it is possible to get a better handle on the extinction towards a star or supernova. Krisciunas et al. (2000) found that SN Ia with mid-range decline rates exhibited uniform V *minus* near-IR colors from $-9 \lesssim t - T(B_{max}) \lesssim +27$ d, allowing a determination of the V *minus* near-IR color excesses and a more robust estimate of A_V. Krisciunas et al. (2004b) showed that slowly declining SN Ia have V *minus* near-IR colors roughly 0.24 mag bluer than those of mid-range decliners.

Fig. 8 shows that no simple vertical shifting of our V *minus* near-IR templates matches the SN 1999ac data from $-9 \lesssim t - T(B_{max}) \lesssim +27$ d. If, however, we restrict the fits to the first 20 days after $T(B_{max})$, we obtain color excesses of $E(V - J_s) = 0.44 \pm 0.08$, $E(V - H) = 0.47 \pm 0.06$, and $E(V - K_s) = 0.37 \pm 0.06$. As discussed above in §2.3, the best behaved photometric band before and after the time of maximum light was K_s. Since the V-band data in the first weeks after maximum is also well behaved, we would suggest that the most reliable color index from which to derive a color excess and extinction is $V - K_s$. With $A_V = 1.129 \pm 0.029 \times E(V - K_s)$ based on the reddening model of Cardelli, Clayton, & Mathis (1989), we obtain $A_V(\mathrm{tot}) = 0.42 \pm 0.07$ mag. This implies $E(B - V)_{host} = 0.09$, slightly less than we obtained from optical photometry only. We shall adopt this smaller value as the best estimate of the host galaxy color excess.

According to Theureau et al. (1998) the heliocentric radial velocity of the host of SN 1999ac is 2847 km s^{-1}. Corrected to the frame of the Cosmic Microwave Background radiation, this velocity is 2942 km s^{-1}. With a Hubble constant of 72 km s^{-1} Mpc^{-1} (Freedman et al. 2001) we get a distance modulus of $m - M = 33.06 \pm 0.22$ mag, where the uncertainty corresponds to a random velocity of $\pm$300 km s^{-1}. If $V_{max} = 14.20 \pm 0.02$ and $A_V = 0.42 \pm 0.07$ mag, the absolute magnitude of SN 1999ac is -19.28 ± 0.24. This is 0.24 mag brighter than the value given by Li et al. (2003), who assumed zero host galaxy reddening on the basis of the position of the SN in its host and the lack of Na I D absorption in the spectra (Li 2005, private communication). The absolute magnitude at maximum can be compared to $M_V = -19.13$ for a typical SN Ia with $\Delta m_{15}(B) = 1.33$ and $H_0 = 72$ (Phillips et al. 1999, Eqn. 18).

The absolute magnitudes of SN 1999ac depend critically on the adopted host galaxy extinction. While this problem is potentially unsolveable in the case of optical absolute magnitudes, serious systematic errors in the extinction corrections are less problematic in the near-IR. Table 1 and Fig. 3 of Krisciunas, Phillips, & Suntzeff (2004a) adopt total $VJHK$ extinctions of 0.51, 0.14, 0.10, and 0.06 mag, respectively, and show that the near-

---

Krisciunas et al. 2004c).

IR absolute magnitudes of SN 1999ac are statistically equal to the mean of SN Ia with slower decline rates.

4.2. Luminosity and Bolometric Light Curve

In Fig. 13 we show the bolometric light curves of SNe 1994D, 1999aa, and 1999ac, calculated using the $UBVRI$ photometry of Jha (2002), and our $BVRI$ photometry. For details on the method see Suntzeff (2003). As stated above, we assumed a distance modulus $m - M = 33.06$ mag and $\mathrm{E}(B-V)_{host} = 0.09$ mag for SN 1999ac. The three objects represented in Fig. 13 have essentially the same peak bolometric luminosity. While SNe 1994D and 1999ac have the same observed B-band decline rates, their bolometric decline rates are clearly different.

Candia et al. (2003) considered the difference of log L at maximum compared to log L at 90 days after maximum. Calling this parameter $\Delta\log_{10}$ L_{90}, Candia et al. (2003) found that it correlates with $\Delta\mathrm{m}_{15}(B)$, which allowed them to gain insight into the nature of the effective decline rate of the peculiar SN 2000cx. Both SNe 1999aa and 1999ac have $\Delta\log_{10}$ $\mathrm{L}_{90} \approx 1.40$. Taken altogether, the evidence suggests that SN 1999ac was energetically much more similar to the spectroscopically peculiar slow decliner SN 1999aa than to the faster declining SN 1994D.

Finally, in Fig. 14 we show the equivalent of the luminosity vs. decline rate relation for SN Ia, but using bolometric light curves. The ordinate is the logarithm of the peak luminosity, while the abscissa represents the decline in log L over the first 15 days after the bolometric maximum. SN 1999ac had a peak bolometric luminosity and bolometric decline rate near the mid-range of most of the objects represented. Except for the record-setting slow decliner SN 2001ay (Nugent et al. 2006) and the faster declining SNe 1992A (Hamuy et al. 1996b) and 1999by (Garnavich et al. 2004), SNe Ia appear to occupy a rather small parameter space in the bolometric decline rate graph. This argues in favor of a uniform explosion mechanism for the majority of Type Ia supernovae.

5. Conclusions

The Type Ia supernova 1999ac was peculiar in several respects. As shown by Garavini et al. (2005) and by our data, the spectra of SN 1999ac resembled the unusual SN 1999aa at early times. From maximum light onward, however, the spectrum was essentially normal. This underscores a thorny issue of SN classification: if early-time spectra are not obtained,

there may be no way to determine if a particular Type Ia supernova is unusual (see also Li et al. 2001a).

The optical photometry of SN 1999ac was unusual in that it had a slow rise rate (like SN 1991T), but a much more rapid B-band decline rate (like SN 1994D). In this sense it was the opposite of SN 2000cx, which was a rapid riser, but slow decliner. This is in striking contrast to the B- and V-band light curves of most SN Ia which can be characterized by a single stretch factor (Goldhaber et al. 2001). In the case of SN 1999ac, our best estimate of the extinction is obtained from the $V - K_s$ colors during the first 20 days after T(B_{max}). We find A_V(tot) = 0.42 mag, implying a non-zero host galaxy reddening of E$(B-V)_{host}$ = 0.09 mag.

In spite of the peculiar photometric properties of SN 1999ac, because near-infrared extinction corrections are an order of magnitude smaller than at optical wavelengths, the infrared absolute magnitudes of SN 1999ac cannot be systematically in error by more than a few hundredths of a magnitude. The derived infrared absolute magnitudes (Krisciunas, Phillips, & Suntzeff 2004a) are statistically equal to the mean of all other SN Ia with slower decline rates. As a result, the unusual SN 1999ac can still be regarded as an infrared standard candle. Its J_sHK_s light curves were very similar to those of the normal SN 2001el.

The bolometric light curve of SN 1999ac closely resembled that of the spectroscopically peculiar slow decliner SN 1999aa. The differences of their bolometric luminosities at maximum compared to 90 days after maximum are almost identical. As measured by this parameter, SN 1999ac behaved as if it were a slow decliner. Hence, in terms of its energetics and pre-maximum spectral characteristics, there is little doubt that SN 1999ac was closely related to other peculiar, slow-declining events such as SNe 1999aa and 1991T.

Finally, we have also examined the luminosity vs. decline rate relation for SN Ia, but considered according to their bolometric light curves. Most events occupy a rather small parameter space, suggesting a uniform explosion mechanism for these supernovae.

M. Hamuy and G. Galaz acknowledge the support of Fondap Center for Astrophysics grant number 15010003. Some of the observations were obtained with the Yale 1 m telescope at CTIO, operated by the Yale/AURA/Lisbon/OSU (YALO) consortium, now the Small and Moderate Aperture Research Telescope System (SMARTS) Consortium. We acknowledge funding from STScI from the grants GO-8243.02-A and GO-8648.10-A. We made use of data in the NASA/IPAC Extragalactic Database (NED). We thank Max Stritzinger for discussions relating to bolometric light curves, and Weidong Li for facilitating his published spectra of

SN 1999aa.

REFERENCES

Barris, B. J., Tonry, J. L., Blondin, S., et al. 2004, ApJ, 602, 571

Benetti, S., Meikle, P., Stehle, M., et al. 2004, MNRAS, 348, 261

Bennett, C. L., Halpern, M., Hinshaw, G., et al. 2003, ApJS, 148, 1

Benetti, S., Cappellaro, E., Mazzali, P. A., et al. 2005, ApJ, 623, 1011

Bessell, M. S. 1979, PASP, 91, 589

Bessell, M. S. 1990, PASP, 102, 1181

Branch, D. 2001, PASP, 113, 169

Branch, D., Fisher, A. & Nugent, P. 1993, AJ, 106 2383

Candia, P., Krisciunas, K., Suntzeff, N. B., et al. 2003, PASP, 115, 277

Cardelli, J. A., Clayton, G. C., & Mathis, J. S. 1989, ApJ, 345, 245

Cristiani, S., Cappellaro, E., Turatto, M., et al. 1992, A&A, 259, 63

Elias, J. H., Frogel, J. A., Hackwell, J. A., & Persson, S. E. 1981, ApJ, 251, L13

Elias, J. H., Matthews, G., Neugebauer, G., & Persson, S. E. 1985, ApJ, 296, 379

Filippenko, A. V., Richmond, M. W., Matheson, T., et al. 1992a, ApJ, 384, 15

Filippenko, A. V., Richmond, M. W., Branch, D., et al. 1992b, AJ, 104, 1543

Filippenko, A. V., Li, W. D., & Leonard, D. C. 1999, IAU Circ., 7108

Freedman, W. L., Madore, B. F., Gibson, B. K., et al. 2001, ApJ, 553, 47

Garavini, G., Folatelli, G., Goobar, A., et al. 2004, AJ, 128, 387

Garavini, G., Aldering, G., Amadon, A., et al. 2005, AJ, 130, 2278

Garnavich, P. M., Kirshner, R. P., Challis, P., et al. 1998, ApJ, 493, 53

Garnavich, P. M., Bonanos, A. Z., Krisciunas, K., et al. 2004, ApJ, 613, 1120

Gibson, B. K., Stetson, P. B., Freedman, W. L., et al. 2000, ApJ, 529, 723

Gibson, B. K., & Stetson, P. B. 2001, ApJ, 547, L103

Goldhaber, G., Groom, D. E., Kim A., et al. 2001, ApJ, 558, 359

Guy, J., Astier, P., Nobili, S., Regnault, N., & Pain, R. 2005, A&A, 443, 781

Hamuy, M., Phillips, M. M., Suntzeff, N. B., Schommer, R. A., Maza, J., & Avilés, R. 1996a, AJ, 112, 2398

Hamuy, M., Phillips, M. M., Suntzeff, N. B., Schommer, R. A., Maza, J., Smith, R. C., Lira, P., & Avilés, R. 1996b, AJ, 112, 2438

Hamuy, M., Maza, J., Pinto, P. A., et al. 2002, AJ, 124, 417

Hernandez, M., Meikle, W. P. S., Aparicio, A., et al. 2000, MNRAS, 319, 223

Jha, S., Garnavich, P. M., Kirshner, R. P., et al. 1999, ApJS, 125, 73

Jha, S. 2002, Ph. D. thesis, Harvard University (Photometric data and transformations between stretch factors and $\Delta m_{15}(B)$ might be more easily obtained from Jha et al. 2006, AJ, 131, 527.)

Knop, R. A., Aldering, G., Amanullah, R., et al. 2003, ApJ, 598, 102

Krisciunas, K., Hastings, N. C., Loomis, K., McMillan, R., Rest, A., Riess, A. G., & Stubbs, C. 2000, ApJ, 539, 658

Krisciunas, K., Phillips, M. M., Stubbs, C., et al. 2001, AJ, 122, 1616

Krisciunas, K., Suntzeff, N. B., Candia, P., et al. 2003, AJ, 125, 166

Krisciunas, K., Phillips, M. M., & Suntzeff, N. B. 2004a, ApJ, 602, L81

Krisciunas, K., Phillips, M. M., Suntzeff, N. B., et al. 2004b, AJ, 127, 1664

Krisciunas, K., Suntzeff, N. B., Phillips, M. M., et al. 2004c, AJ, 128, 3034

Krisciunas, K., Garnavich, P. M., Challis, P., et al. 2005, AJ, 130, 2453

Landolt, A. U. 1992, AJ, 104, 340

Leibundgut, B. 2000, Astron. Ap. Rev., 10, 179

Leibundgut, B., Kirshner, R. P., Phillips, M. M., et al. 1993, AJ, 105, 301

Li, W. D., Filippenko, A. V.. Treffers, R. R., Riess, A. G., Hu, J., Qiu, Y. 2001a, ApJ, 546, 734

Li, W. D., Filippenko, A. V., Gates, E., et al. 2001b, PASP, 113, 1178

Li, W. D., Filippenko, A. V., Chornock, R., et al. 2003, PASP, 115, 453

Lira, P. 1995, Master's thesis, Univ. Chile

Lira, P., Suntzeff, N. B., Phillips, M. M., et al. 1998, AJ, 115, 234

Livio, M. 2000, in The Greatest Explosions since the Big Bang: Supernovae and Gamma-Ray Bursts, eds. M. Livio, N. Panagia, & K. Sahu (Baltimore, Maryland: Space Telescope Science Institute), 334

Maza, J., Hamuy, M., Phillips, M. M., Suntzeff, N. B., Avilés, R. 1994, ApJ, 424, 107

Mazzali, P. A., Chugai, N., Turatto, M., Lucy, L. B., Danziger, I. J., Cappellaro, E., della Valle, M., & Benetti, S. MNRAS, 284 151

Meikle, W. P. S. 2000, MNRAS, 314, 782

Modjaz, M., King, J. Y., Papenkova, M., Friedman, A., Johnson, R. A., Li, W. D., Treffers, R. R., & Fililppenko, A. V. 1999, IAU Circ., 7114

Nobili, S., Goobar, A., Knop, R., & Nugent, P. 2003, A&A, 404, 901

Nobili, S., Amanullah, R., Garavini, G., et al. 2005, A&A, 437, 789

Nugent, P., Phillips, M., Baron, E., Branch, D., Hauschildt, P. 1995, ApJ, 455, 147

Nugent, P., et al. 2006, in preparation

Olsen, E. H. 1983, A&AS, 54, 55

Parodi, B. R., Saha, A., Sandage, A., & Tammann, G. A. 2000, ApJ, 540, 634

Perlmutter, S., Gabi, S., Goldhaber, G., et al. 1997, ApJ, 483, 565

Perlmutter, S., Aldering, G., Goldhaber, G., et al. 1999, ApJ, 517, 565

Persson, S. E., Murphy, D. C., Krzeminski, W., Roth, M., & Rieke, M. J. 1998, AJ, 116, 2475

Phillips, M. M. 1993, ApJ, 413, L105

Phillips, M. M., Phillips, A. C., Heathcote, S. R., et al. 1987, PASP, 99, 592

Phillips, M. M., Wells, L. A., Suntzeff, N. B., Hamuy, M., Leibundgut, B., Kirshner, R. P., & Foltz, C. B., AJ, 103, 1632

Phillips, M. M., & Kunkel, W. 1999, IAU Circ., 7122

Phillips, M. M., Lira, P., Suntzeff, N. B., Schommer, R. A., Hamuy, M., & Maza, J. 1999, AJ, 118, 1766

Phillips, M. M., et al. 2003, in From Twilight to Highlight: The Physics of Supernovae, eds. W. Hillebrandt & B. Leibundgut (Berlin: Springer-Verlag), 193

Pinto, P. A., & Eastman, R. G. 2000a, ApJ, 530, 744

Pinto, P. A., & Eastman, R. G. 2000b, 530, 757

Riess, A. G., Press, W. H., & Kirshner, R. P. 1996, ApJ, 473, 88

Riess, A. G., Filippenko, A. V., Challis, P., et al. 1998, AJ, 116, 1009

Riess, A. G., Nugent, P. E., Gilliland, R. L., et al. 2001, ApJ, 560, 49

Riess, A. G., et al., 2004, ApJ, 607, 665

Riess, A. G., Li, W. D., Stetson, P. B., et al. 2005, ApJ, 627, 579

Saha, A., Sandage, A., Thim, F., Labhardt, L., Tammann, G. A., Christensen, J., Panagia, N., & Macchetto, F. D. 2001, ApJ, 551, 973

Sandage, A., Saha, A., Tammann, G. A., Labhardt, L., Panagia, N., & Macchetto, F. D. 1996, ApJ, 460, 15

Schlegel, D. J., Finkbeiner, D. P., & Davis, M. 1998, ApJ, 500, 525

Serkowski, K. 1970, PASP, 82, 908

Sneden, C., Gehrz, R. D., Hackwell, J. A., York, D. G., & Snow, T. P. 1978, ApJ, 223, 168

Stetson, P. 1987, PASP, 99, 191

Stetson, P. 1990, PASP, 102, 932

Stritzinger, M., Hamuy, M., Suntzeff, N. B., et al. 2002, AJ, 124, 2100

Suntzeff, N. B. 1996, IAU Colloq. 145, Supernovae and Supernova Remnants, ed. R. McCray & Z. Wang (New York: Cambridge Univ. Press), 41

Suntzeff, N. B., Phillips, M. M., Covarrubias, R., et al. 1999, AJ, 117, 1175

Suntzeff, N. B. 2000, in AIP Conf. Proc. 522, Cosmic Explosions, eds. S. S. Holt & W. W. Zhang (Melville, NY: AIP), 65

Suntzeff, N. B., in Proc. ESO/MPA/MPE Workshop, From Twilight to Highlight – the Physics of Supernovae, ed. W. Hillebrandt & B. Leibundgut (Berlin: Springer), 183

Theureau, G., Bottinelli, L., Coudreau-Durand, N., Gouguenheim, L., Hallet, N., Loulergue, M., Paturel, G., & Teerikorpi, P., A&AS, 130, 333

Tonry, J. L., Schmidt, B. P., Barris, B., et al. 2003, ApJ, 594, 1

Tripp, R., & Branch, D. 1999, ApJ, 525, 209

Turatto, M., Benetti, S., Cappellaro, E., Danziger, I. J., della Valle, M., Gouiffes, C., Mazzali, P. A., & Patat, F., MNRAS, 283, 1

Walker, G. A. H., Andrews, D. H., Hill, G., Morris, S. C., Smyth, W. G., & White, J. R. 1971, Pub. Dominion Astophys. Obs., 13, 415

Table 1. Optical Photometric Sequence near SN 1999ac[a]

Star ID[b]	V	$B-V$	$V-R_{KC}$	$V-I_{KC}$	N_V	N_{B-V}	$N_{V-R_{KC}}$	$N_{V-I_{KC}}$
1	15.839 (0.004)	1.119 (0.009)	0.615 (0.005)	1.185 (0.005)	11	12	12	12
2	17.359 (0.007)	1.485 (0.035)	1.001 (0.008)	2.102 (0.009)	9	10	10	10
3	16.193 (0.004)	0.747 (0.010)	0.412 (0.007)	0.789 (0.007)	11	12	12	12
4	16.889 (0.007)	0.662 (0.012)	0.415 (0.010)	0.801 (0.009)	10	11	11	12
5	13.776 (0.002)	0.739 (0.003)	0.403 (0.003)	0.759 (0.003)	11	12	12	12
6	17.814 (0.008)	0.992 (0.027)	0.571 (0.013)	1.104 (0.011)	7	9	10	10
7	14.767 (0.002)	0.680 (0.006)	0.388 (0.004)	0.757 (0.004)	10	11	11	11
8	17.222 (0.007)	0.672 (0.016)	0.426 (0.009)	0.839 (0.011)	8	10	10	10
9	17.414 (0.009)	0.627 (0.014)	0.362 (0.015)	0.745 (0.011)	9	10	10	10
11	18.056 (0.016)	0.709 (0.039)	0.426 (0.023)	0.821 (0.022)	4	8	8	8
12	18.730 (0.020)	0.951 (0.077)	0.552 (0.029)	1.117 (0.032)	2	4	4	4
13	17.920 (0.021)	1.451 (0.034)	0.892 (0.025)	1.821 (0.025)	2	3	3	3
17	17.896 (0.016)	0.625 (0.025)	0.369 (0.037)	0.741 (0.022)	2	2	2	2
19	17.259 (0.020)	0.794 (0.027)	0.455 (0.022)	0.906 (0.025)	3	3	3	3
20	17.990 (0.010)	0.771 (0.018)	0.444 (0.016)	0.890 (0.014)	7	7	7	7
21	18.565 (0.025)	1.629 (0.092)	1.168 (0.029)	2.671 (0.027)	2	4	4	4
22	17.165 (0.006)	0.830 (0.024)	0.452 (0.009)	0.909 (0.010)	6	6	6	6
23	17.925 (0.018)	0.559 (0.027)	0.344 (0.022)	0.706 (0.023)	4	4	4	4
24	17.989 (0.016)	0.798 (0.104)	0.504 (0.035)	0.984 (0.031)	2	2	2	2

[a]In this and subsequent tables the numbers in parentheses are the 1σ uncertainties.

[b]The identifications are the same as in Fig. 1.

Table 2. $BV(RI)_{KC}$ Photometry of SN 1999ac

JD−2,450,000	UT Date[a]	B	V	R_{KC}	I_{KC}	Observer+Telescope
1238.90	Mar01.40	15.485 (0.013)	15.487 (0.008)	15.444 (0.013)	15.415 (0.016)	Germany CTIO 0.9 m
1239.90	Mar02.40	15.285 (0.012)	15.294 (0.007)	15.255 (0.012)	15.228 (0.015)	Germany CTIO 0.9 m
1240.89	Mar03.40	15.106 (0.015)	15.125 (0.009)	15.082 (0.020)	15.055 (0.023)	Germany CTIO 0.9 m
1241.87	Mar04.37	15.039 (0.026)	14.901 (0.014)	···	14.802 (0.027)	Espinoza/Gonzalez CTIO YALO 1 m
1243.88	Mar06.38	14.763 (0.028)	14.636 (0.009)	···	14.521 (0.021)	Espinoza/Gonzalez CTIO YALO 1 m
1246.85	Mar09.35	14.480 (0.033)	14.336 (0.022)	···	14.233 (0.053)	Espinoza/Gonzalez CTIO YALO 1 m
1252.85	Mar15.35	14.386 (0.020)	14.136 (0.012)	···	14.286 (0.018)	Espinoza/Gonzalez CTIO YALO 1 m
1257.88	Mar20.38	14.689 (0.014)	14.326 (0.001)	14.248 (0.006)	14.523 (0.004)	Strolger CTIO 0.9 m
1263.83	Mar26.33	15.418 (0.028)	14.618 (0.015)	···	14.706 (0.023)	Espinoza/Gonzalez CTIO YALO 1 m
1266.88	Mar29.38	15.739 (0.028)	14.888 (0.011)	14.678 (0.019)	14.783 (0.016)	Strolger CTIO 0.9 m
1267.91	Mar30.41	15.841 (0.025)	14.952 (0.009)	14.715 (0.016)	14.764 (0.016)	Strolger CTIO 0.9 m
1274.89	Apr06.39	16.353 (0.031)	15.268 (0.014)	14.890 (0.023)	14.792 (0.022)	Strolger CTIO 0.9 m
1275.86	Apr07.36	16.355 (0.023)	15.297 (0.007)	14.904 (0.011)	14.812 (0.016)	Strolger CTIO 0.9 m
1277.86	Apr09.36	16.512 (0.020)	15.386 (0.007)	14.987 (0.017)	14.821 (0.017)	C.Smith/Strolger CTIO 1.5 m
1284.78	Apr16.29	16.917 (0.025)	15.824 (0.017)	15.415 (0.028)	15.104 (0.036)	M.T.Ruiz CTIO 0.9 m
1285.84	Apr17.34	17.001 (0.034)	15.912 (0.009)	···	15.164 (0.015)	Krisciunas/Hastings APO 3.5m
1287.81	Apr19.31	17.088 (0.021)	16.023 (0.013)	15.623 (0.023)	15.316 (0.027)	Germany CTIO 0.9 m
1291.88	Apr23.38	17.222 (0.088)	16.194 (0.050)	15.834 (0.097)	15.565 (0.076)	Strolger/C.Smith/R.Smith CTIO 1.5 m
1294.76	Apr26.26	17.300 (0.055)	16.287 (0.017)	···	15.689 (0.046)	Espinoza/Gonzalez CTIO YALO 1 m
1296.73	Apr28.23	17.361 (0.019)	16.362 (0.012)	16.062 (0.022)	15.807 (0.020)	Strolger/C.Smith/Bonati CTIO 1.5 m
1297.71	Apr29.21	17.327 (0.030)	16.357 (0.012)	···	15.840 (0.041)	Espinoza/Gonzalez CTIO YALO 1 m
1300.60	May02.10	17.460 (0.070)	16.403 (0.029)	···	15.921 (0.093)	Espinoza/Gonzalez CTIO YALO 1 m
1304.79	May06.29	17.523 (0.016)	16.562 (0.009)	16.298 (0.014)	16.134 (0.015)	Strolger CTIO 1.5 m
1305.82	May07.32	17.511 (0.005)	16.581 (0.002)	16.338 (0.006)	16.185 (0.010)	Strolger CTIO 1.5 m
1306.83	May08.33	17.528 (0.032)	16.586 (0.017)	···	16.146 (0.043)	Espinoza/Gonzalez CTIO YALO 1 m
1313.83	May15.33	17.670 (0.028)	16.788 (0.004)	16.605 (0.008)	···	Krisciunas/McMillan APO 3.5
1314.75	May16.25	17.683 (0.017)	16.801 (0.008)	16.608 (0.015)	···	Germany CTIO 0.9 m
1315.72	May17.22	17.688 (0.023)	16.817 (0.010)	···	16.473 (0.021)	Espinoza/Gonzalez CTIO YALO 1 m
1316.83	May18.33	17.711 (0.020)	16.855 (0.012)	16.688 (0.022)	16.554 (0.018)	Krisciunas/McMillan APO 3.5m
1318.68	May20.19	17.755 (0.028)	16.863 (0.018)	···	16.609 (0.029)	Espinoza/Gonzalez CTIO YALO 1 m
1329.68	May31.18	17.892 (0.038)	17.088 (0.017)	···	16.909 (0.046)	Espinoza/Gonzalez CTIO YALO 1 m
1336.64	Jun07.14	17.997 (0.024)	17.266 (0.011)	···	17.192 (0.044)	Espinoza/Gonzalez CTIO YALO 1 m
1363.60	Jul04.10	18.460 (0.025)	17.940 (0.013)	18.118 (0.025)	18.169 (0.039)	Germany CTIO 0.9 m
1364.57	Jul05.07	18.439 (0.032)	17.952 (0.019)	18.105 (0.034)	18.214 (0.044)	Germany CTIO 0.9 m
1365.60	Jul06.10	18.489 (0.021)	17.973 (0.012)	18.130 (0.021)	18.204 (0.029)	Germany CTIO 1.5 m
1375.51	Jul16.01	18.618 (0.031)	18.184 (0.018)	···	···	Corwin CTIO 0.9 m
1379.50	Jul20.00	18.698 (0.044)	18.240 (0.024)	18.469 (0.041)	18.540 (0.052)	Corwin CTIO 0.9 m
1381.52	Jul22.02	18.722 (0.040)	18.273 (0.022)	18.518 (0.038)	···	Corwin CTIO 0.9 m
1382.49	Jul22.99	18.724 (0.044)	18.306 (0.024)	18.565 (0.040)	18.570 (0.053)	Corwin CTIO 0.9 m

[a]Year is 1999.

Table 3. Infrared Photometric Sequence near SN 1999ac

Star ID[a]	J_s	H	K_s
1	13.804 (0.003)	13.183 (0.005)	13.087 (0.008)
2	14.126 (0.008)	13.482 (0.016)	13.256 (0.015)
6	16.167 (0.049)	15.694 (0.043)	15.585 (0.086)
8	15.869 (0.013)	14.440 (0.013)	15.403 (0.015)
9	16.303 (0.040)	16.061 (0.039)	16.010 (0.029)
IR3	15.966 (0.005)	15.427 (0.013)	15.192 (0.017)
IR7	17.093 (0.026)	16.540 (0.028)	16.299 (0.069)

[a]The identifications are the same as those in Table 1 and Fig. 1.

Table 4. Near Infrared Photometry of SN 1999ac

JD−2,450,000	UT Date[a]	J_s	H	K_s	Observer+Telescope
1237.89	Feb28.39	15.919 (0.019)	15.982 (0.036)	16.040 (0.059)	Galaz LCO 1 m
1239.83	Mar02.33	15.461 (0.040)	15.575 (0.048)	15.497 (0.062)	Galaz LCO 1 m
1242.90	Mar05.40	14.942 (0.015)	15.042 (0.019)	14.900 (0.028)	Galaz LCO 1 m
1243.90	Mar06.40	14.819 (0.015)	14.877 (0.017)	14.806 (0.024)	Galaz LCO 1 m
1244.90	Mar07.40	14.673 (0.020)	14.776 (0.021)	14.773 (0.026)	Galaz LCO 1 m
1246.89	Mar09.39	14.509 (0.021)	14.702 (0.027)	14.527 (0.027)	Galaz LCO 1 m
1247.91	Mar10.41	14.514 (0.020)	14.672 (0.031)	14.536 (0.026)	Galaz LCO 1 m
1252.83	Mar15.33	14.567 (0.019)	14.795 (0.022)	14.621 (0.024)	Phillips LCO 1 m
1253.84	Mar16.34	14.736 (0.021)	14.831 (0.023)	14.638 (0.038)	Phillips LCO 1 m
1254.84	Mar17.34	14.781 (0.018)	14.871 (0.023)	14.652 (0.028)	Phillips LCO 1 m
1255.86	Mar18.36	14.845 (0.020)	14.803 (0.036)	14.690 (0.030)	Roth LCO 1 m
1256.79	Mar19.29	14.946 (0.018)	14.837 (0.023)	14.720 (0.024)	Roth LCO 1 m
1257.84	Mar20.34	15.061 (0.015)	14.777 (0.027)	14.726 (0.037)	Roth LCO 1 m
1258.82	Mar21.32	15.210 (0.021)	14.809 (0.031)	14.761 (0.031)	Roth LCO 1 m
1259.85	Mar22.35	15.329 (0.028)	14.863 (0.029)	14.767 (0.035)	Roth LCO 1 m
1260.78	Mar23.28	15.456 (0.032)	14.835 (0.034)	14.777 (0.034)	Roth LCO 1m
1262.84	Mar25.34	15.599 (0.043)	14.770 (0.026)	14.796 (0.026)	Galaz LCO 2.5 m
1264.88	Mar27.38	15.738 (0.020)	14.759 (0.019)	14.807 (0.020)	Galaz LCO 2.5 m
1266.90	Mar29.40	15.757 (0.023)	14.742 (0.021)	14.727 (0.039)	Galaz LCO 2.5 m
1267.78	Mar30.28	15.742 (0.020)	14.746 (0.028)	14.749 (0.034)	Phillips LCO 2.5 m
1270.82	Apr02.32	15.753 (0.022)	···	···	Muena LCO 1 m
1272.85	Apr04.35	15.858 (0.008)	···	···	Marzke/Persson/Beckett LCO 2.5 m
1273.84	Apr05.34	···	14.845 (0.020)	···	Marzke/Persson/Beckett LCO 2.5 m
1287.83	Apr19.33	16.055 (0.028)	15.377 (0.040)	15.495 (0.042)	Galaz/Hamuy LCO 1 m
1288.87	Apr20.37	16.085 (0.018)	15.396 (0.025)	15.669 (0.050)	Hamuy LCO 1 m
1289.86	Apr21.36	16.170 (0.028)	15.359 (0.025)	15.502 (0.118)	Hamuy LCO 1 m
1290.82	Apr22.32	16.254 (0.032)	15.488 (0.065)	15.737 (0.051)	Phillips LCO 1 m
1291.77	Apr23.27	16.356 (0.026)	15.561 (0.039)	15.984 (0.065)	Roth LCO 1 m
1294.81	Apr26.31	16.539 (0.036)	15.724 (0.029)	15.899 (0.040)	Roth LCO 1 m
1298.66	Apr30.16	···	15.894 (0.053)	···	Ivanov SO 1.5 m
1300.78	May02.28	···	15.969 (0.015)	···	McCarthy/Abraham LCO 2.5 m
1303.71	May05.21	···	···	16.293 (0.040)	Ivanov SO 2.3 m
1313.78	May15.28	18.024 (0.037)	···	···	Firth/Roth/McMahon LCO 2.5 m
1330.63	Jun01.13	···	···	17.231 (0.073)	Hungerford SO 2.3 m

[a]Year is 1999.

Table 5. Observed Maximum Light Data for SN 1999ac

Filter	Epoch (J.D. 2450000+)	Magnitude
B	1251.0 (0.5)	14.27 (0.02)
V	1251.9 (0.5)	14.20 (0.02)
R	1252.0 (0.5)	14.17 (0.02)
I	1249.1 (0.5)	14.29 (0.02)
J_s	1249.2 (0.5)	14.51 (0.04)
H	1248.0 (0.5)	14.67 (0.04)
K_s	1248.5 (1.0)	14.54 (0.04)

Table 6. Optical Spectroscopy of SN 1999ac

			Wavelength		Expansion Velocity (km s^{-1})	
JD−2,450,000	UT Date[a]	Phase[b]	Coverage (Å)	Resolution (Å)	Ca II[c]	Si II[d]
1237.89	Feb28.39	−13	3700-9200	7	18856 (500)	12831 (200)
1248.89	Mar11.39	−2	3580-9270	7	14626 (100)	10747 (100)
1258.88	Mar21.38	+8	3600-9270	7	14189 (100)	9219 (100)
1291.85	Apr23.35	+41	3670-9230	7	11126 (500)	···

[a]Year is 1999.

[b]Number of days with respect to epoch of B-band maximum.

[c]Rest frame wavelength = 3945.1 Å.

[d]Rest frame wavelength = 6355.2 Å.

Fig. 1.— NGC 6063, SN 1999ac, and the field stars nearby. This 7.3 by 7.3 arcmin image was made from multiple V-band exposures obtained with the CTIO 0.9 m telescope shortly after the time of maximum light of the SN.

Fig. 2.— $BVRI$ photometry of SN 1999ac. Data for the various telescopes used are plotted with different symbols, as is also the photometry of Jha (2002).

Fig. 3.— Top Panel – Observed $B-V$, $V-R$, and $V-I$ colors of SN 1999ac. Data for the various telescopes used are plotted with different symbols, as is also the photometry of Jha (2002).

Fig. 4.— BVRI photometry of SN 1999ac compared with the light curves of the Type Ia SNe 1994D ($\Delta m_{15}(B) = 1.32$), 1991T ($\Delta m_{15}(B) = 0.94$), and 1992al ($\Delta m_{15}(B) = 1.11$). The curves have been adjusted to be the same at maximum in each filter. Note that while SN 1999ac and SN 1994D have very similar values (1.33 vs. 1.32) of the decline rate parameter $\Delta m_{15}(B)$, their light curves are not at all identical. Even more striking is the very slow rise to maximum of SN 1999ac as compared to SN 1994D.

Fig. 5.— $B-V$, $V-R$, and $V-I$ colors of SN 1999ac corrected for a color excess E($B-V$) = 0.046 mag due to dust in our Galaxy (Schlegel, Finkbeiner, & Davis 1998) and plotted as a function of the time (in days) since the date of B maximum (see Table 5). Plotted for comparison are similar data for SN 1999aa (Krisciunas et al. 2000) corrected for a Galactic reddening of E($B-V$) = 0.040 (Schlegel, Finkbeiner, & Davis 1998). Shown schematically is the evolution in these three colors of SNe 1994D ($\Delta m_{15}(B) = 1.32$), 1991T ($\Delta m_{15}(B) = 0.94$), and 1992al ($\Delta m_{15}(B) = 1.11$) corrected for the Galactic and host galaxy reddenings given in Table 2 of Phillips et al. (1999). The straight black line shows the Lira (1995) relation for unreddened SNe Ia.

Fig. 6.— J_s, H, and K_s photometry of SN 1999ac, coded by telescope and instrument. For most measurements the uncertainties are less than or equal to the size of the points. Symbols: circles = LCO 1 m; upward pointing triangles = LCO 2.5 m + ClassicCam; downward pointing triangles = LCO 2.5 m + CIRSI; asterisk = Steward Observatory 1.5 m; squares = Steward Observatory 2.3 m. For comparison we have fit higher order polynomials to the light curves of SNe 1998bu, 1999ee and 2001el. All data are plotted with respect to the primary maxima. The photometry also includes small K-corrections interpolated from Table 11 of Krisciunas et al. (2004b). In the time domain we have subtracted off the dates of B-band maximum and corrected for time dilation.

Fig. 7.— Comparison of $BVIJ_sHK_s$ data of SN 1999ac and generic (stretch = 1.00) light curve templates. The data have been scaled in the time axis by stretch factors derived using

$\Delta m_{15}(B) = 1.33$ (Jha 2002) and also taking into account time dilation. So, if the stretched data and a template match, then the stretch factor correctly characterizes the light curve. For the B- and V-band data the stretch factors are 1.175 and 1.128, respectively. For the other filters we used the average of these values, 1.151. The B-band template is from Goldhaber et al. (2001), using a parabolic turn on at -20 d. The V-band template is from Knop et al. (2003). The other maximum-time templates are from Krisciunas et al. (2004b). In the BVI plots the circles are CTIO 0.9-m data, while the triangles are data from Jha (2002). In the J_sHK_s plots the circles are LCO 1-m data, while the triangles are data from the LCO 2.5-m using ClassicCam. If error bars are not shown, they are smaller than or equal to the size of the points. Since the stretched data do not conform well to the $BVIJ_s$ templates, the light curves must be characterized by different stretch factors before and after maximum light.

Fig. 8.— $V - J_s$, $V - H$, and $V - K_s$ color evolution of SN 1999ac. The solid lines are the zero-reddening loci derived by Krisciunas et al. (2000), based on data for eight SNe Ia which are mid-range decliners, and offset by $E(V - J) = 0.44$, $E(V - H) = 0.47$, and $E(V - K) = 0.37$ mag, respectively.

Fig. 9.— Spectra of SN 1999ac obtained at LCO from 13 days before to 41 days after the epoch of B maximum. Identifications of the major contributors to the strongest absorption features in the -2 day spectrum are also indicated. The abscissa corresponds to observer frame wavelengths.

Fig. 10.— Spectrum of SN 1999ac obtained at -13 days is compared with spectra from a similar epoch of SNe 1991T, 1999aa, and 1990N. Identifications of the major contributors to the strongest absorption features are indicated. The abscissa here and in Figs. 11 and 12 corresponds to rest-frame wavelengths.

Fig. 11.— Spectrum of SN 1999ac obtained at -2 days is compared with spectra from a similar epoch of SNe 1991T, 1999aa, and 1990N. Identifications of the major contributors to the strongest absorption features are indicated.

Fig. 12.— Spectrum of SN 1999ac obtained at $+8$ days is compared with spectra from a similar epoch of SNe 1991T and 1990N. Identifications of the major contributors to the strongest absorption features are indicated.

Fig. 13.— Bolometric light curves of SNe 1994D, 1999aa, and 1999ac constructed from $UBVRI$ photometry. The luminosity is measured in erg s^{-1}.

Fig. 14.— Bolometric decline rate relation. For each object we plot the logarithm of the peak luminosity (in erg s^{-1}) vs. the bolometric equivalent of $\Delta m_{15}(B)$, namely the difference

of log L at the maximum compared to 15 days later. SN 1999ac is represented by the (red) circle, while three other specific objects are labelled. The remaining objects, represented by triangles, from left to right are: SNe 1999aw, 1999aa, 1999gp, 1989B, 1990N, 2001el, 1999ee, 1998bu, 1996X, 2000cx, and 1994D.

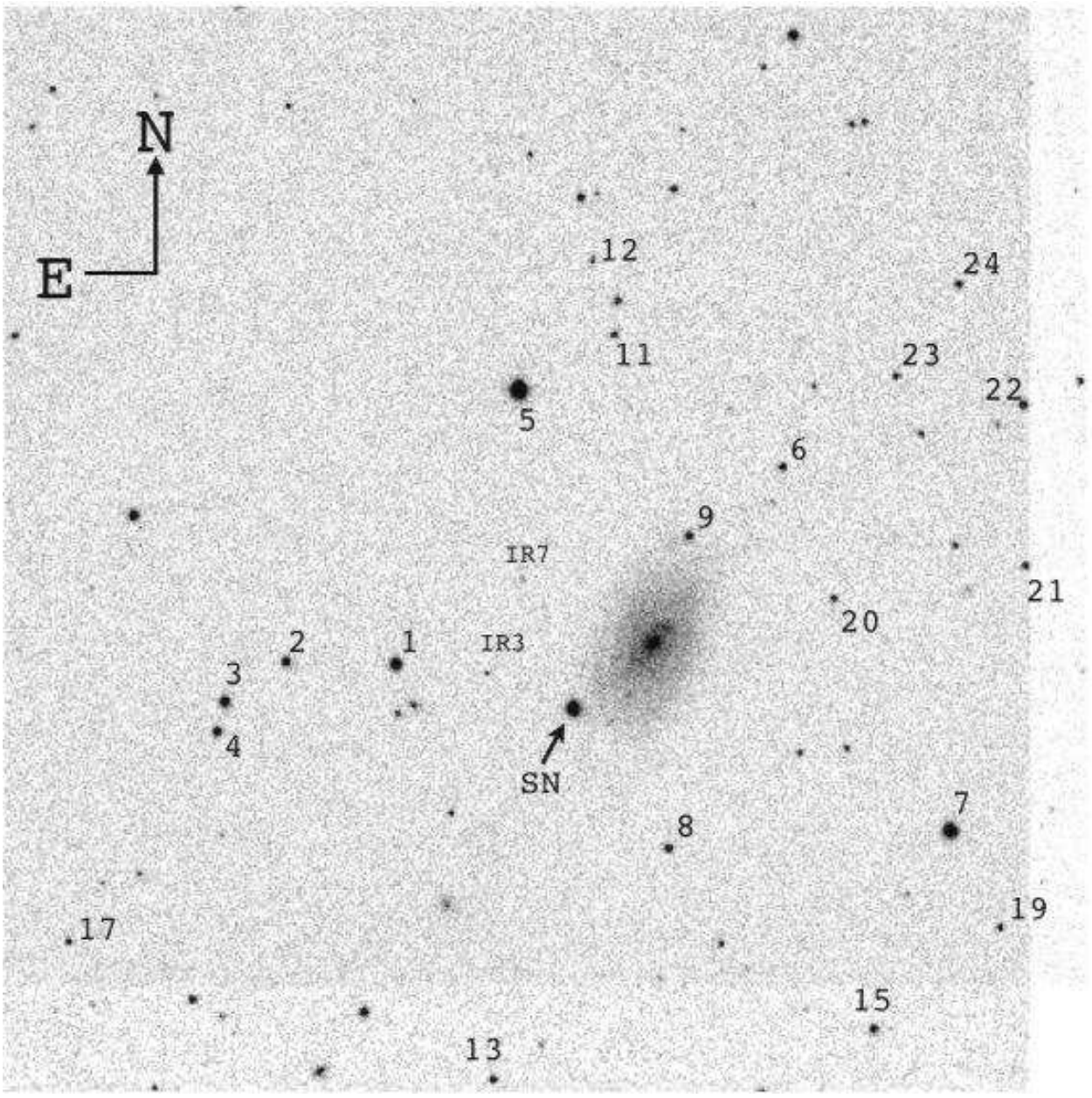

Phillips *et al.* Fig. 1

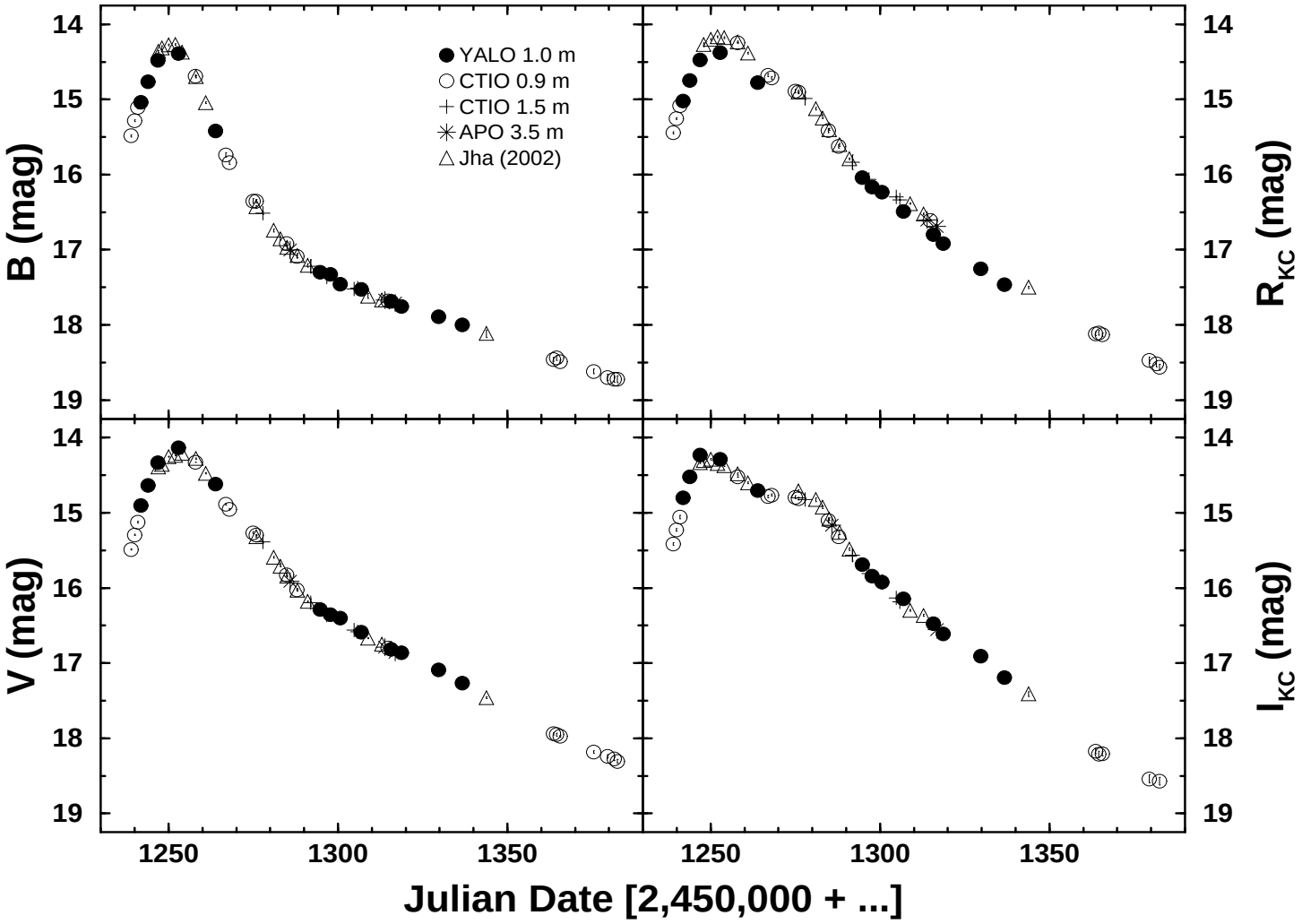

Phillips *et al.* Fig. 2

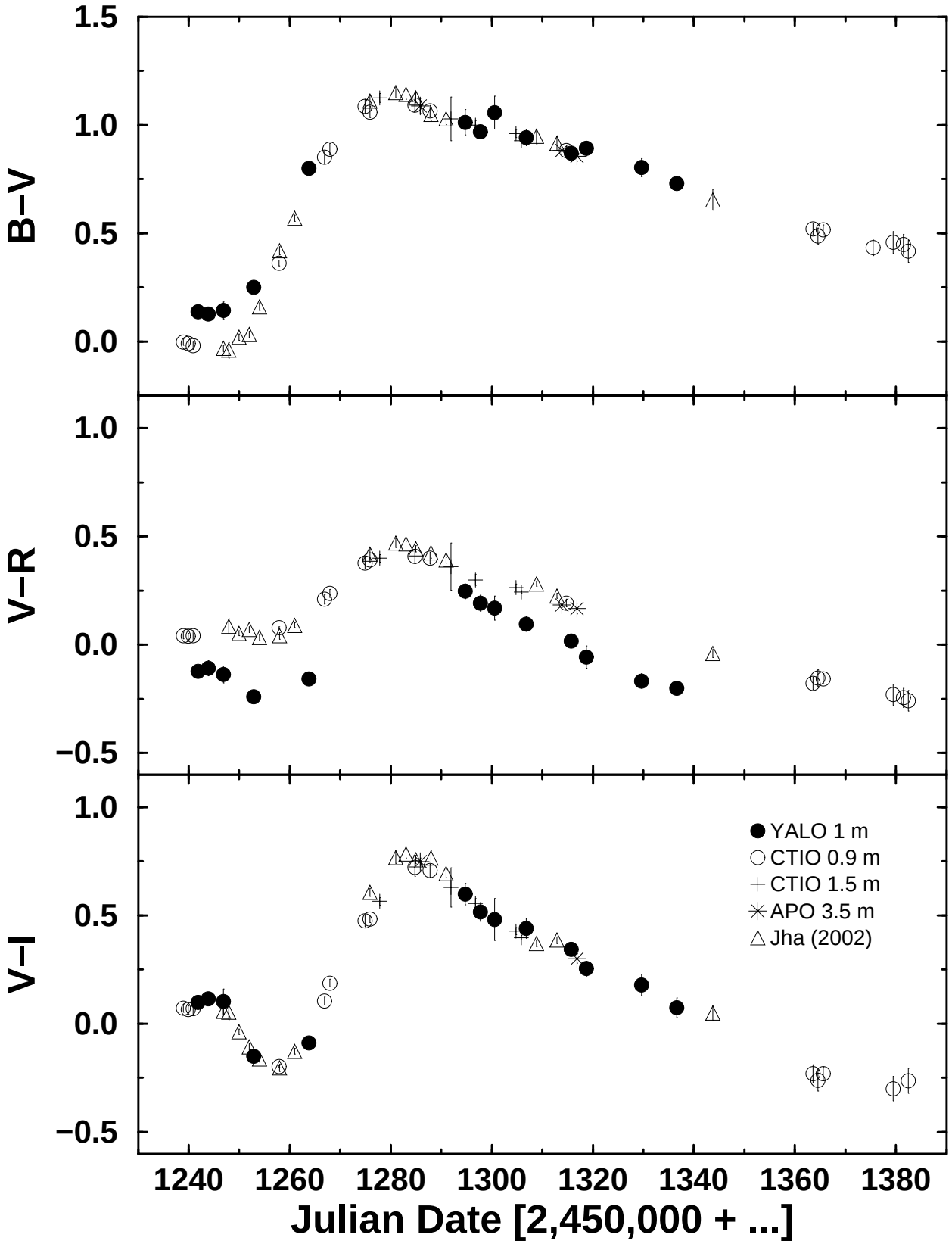

Phillips *et al.* Fig. 3

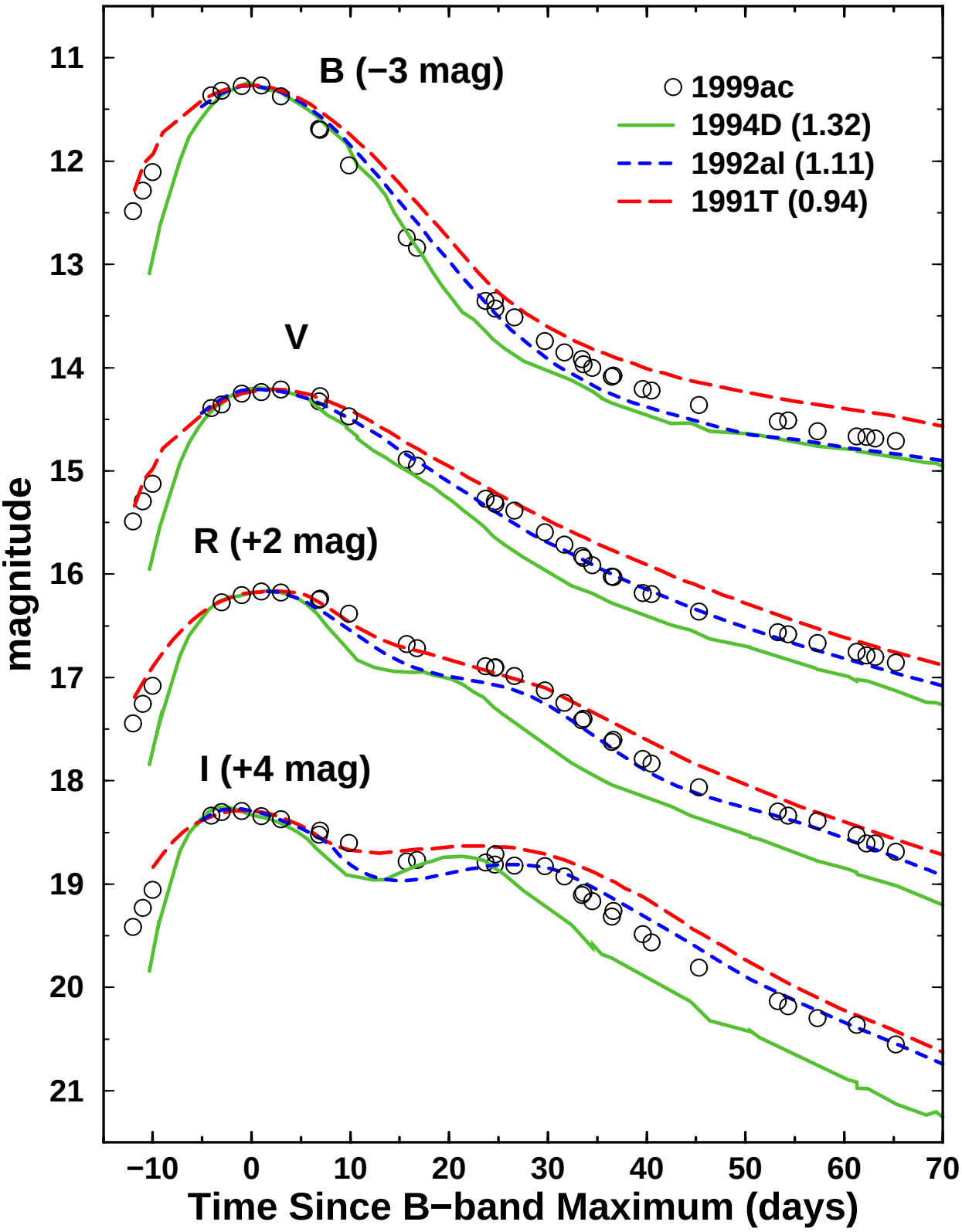

Phillips *et al.* Fig. 4

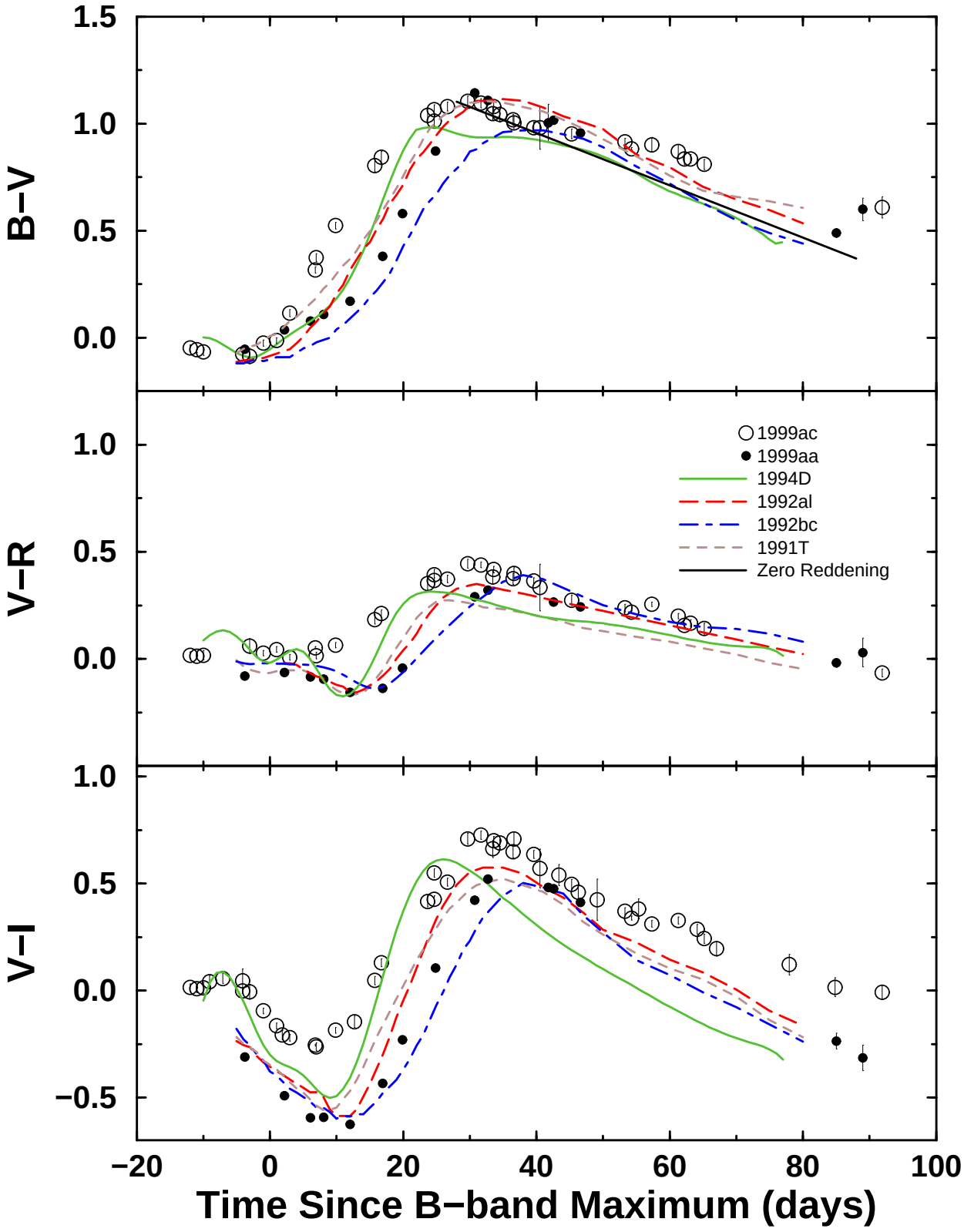

Phillips *et al.* Fig. 5

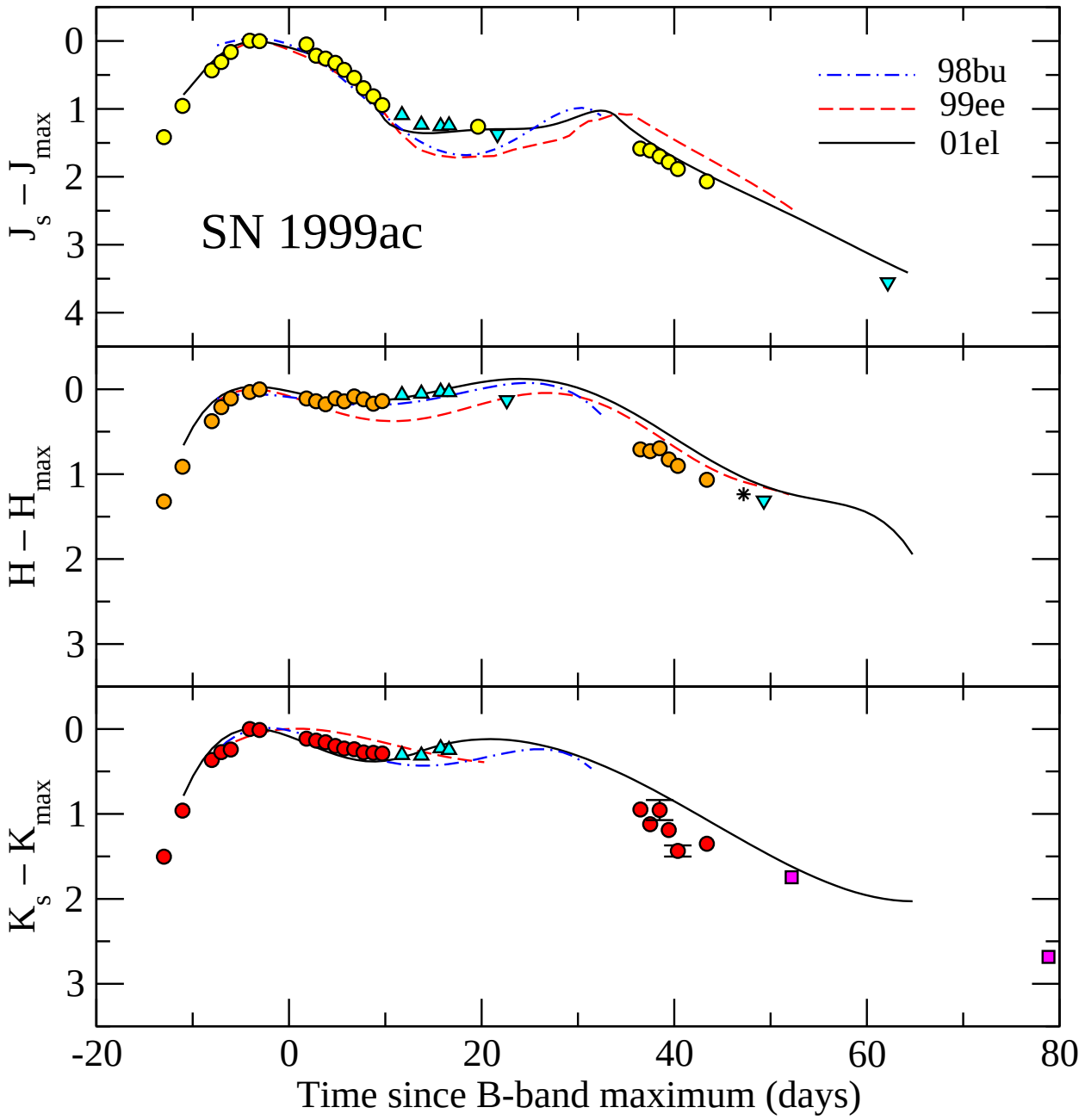

Phillips *et al.* Fig. 6

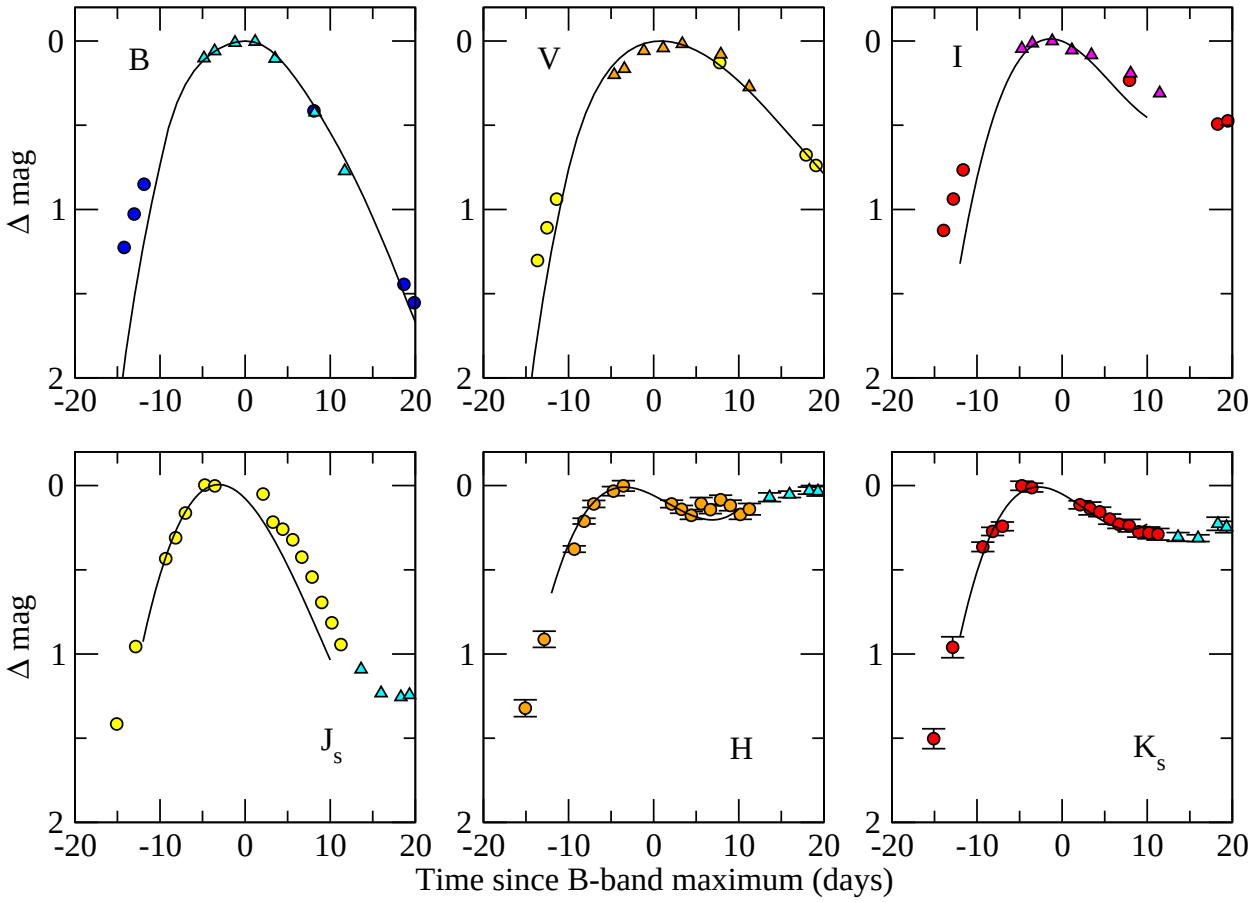

Phillips *et al.* Fig. 7

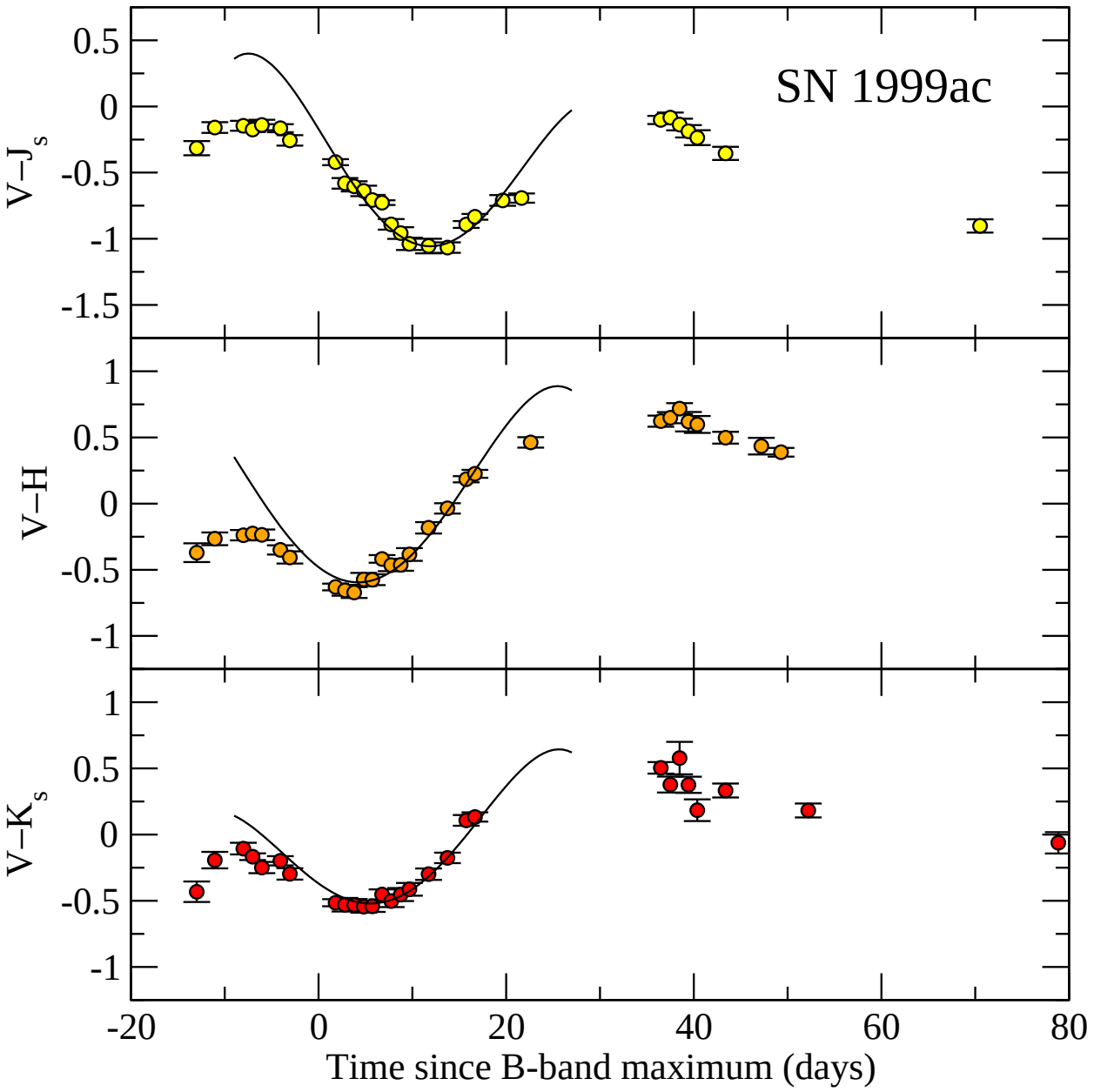

Phillips *et al.* Fig. 8

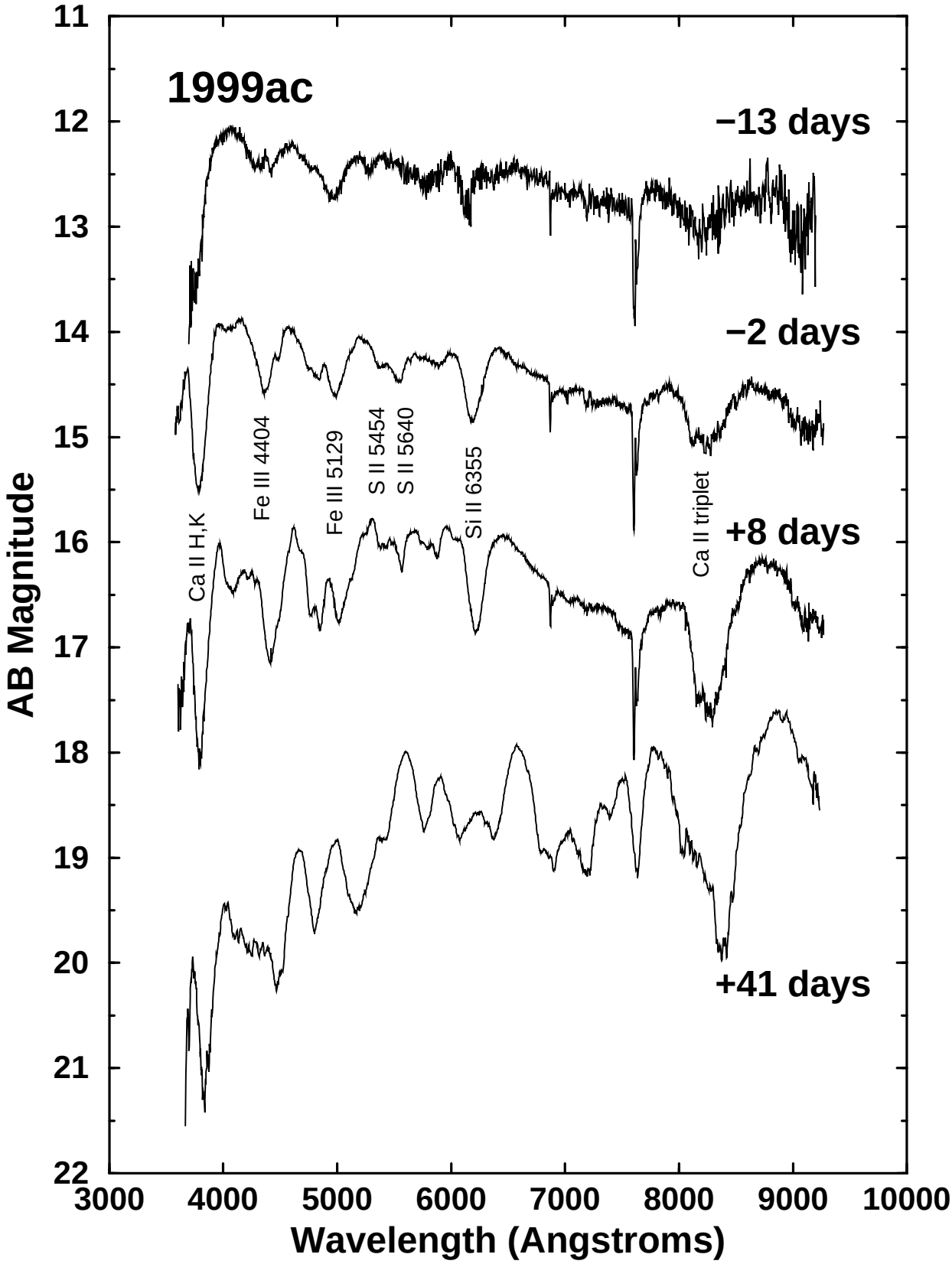

Phillips *et al.* Fig. 9

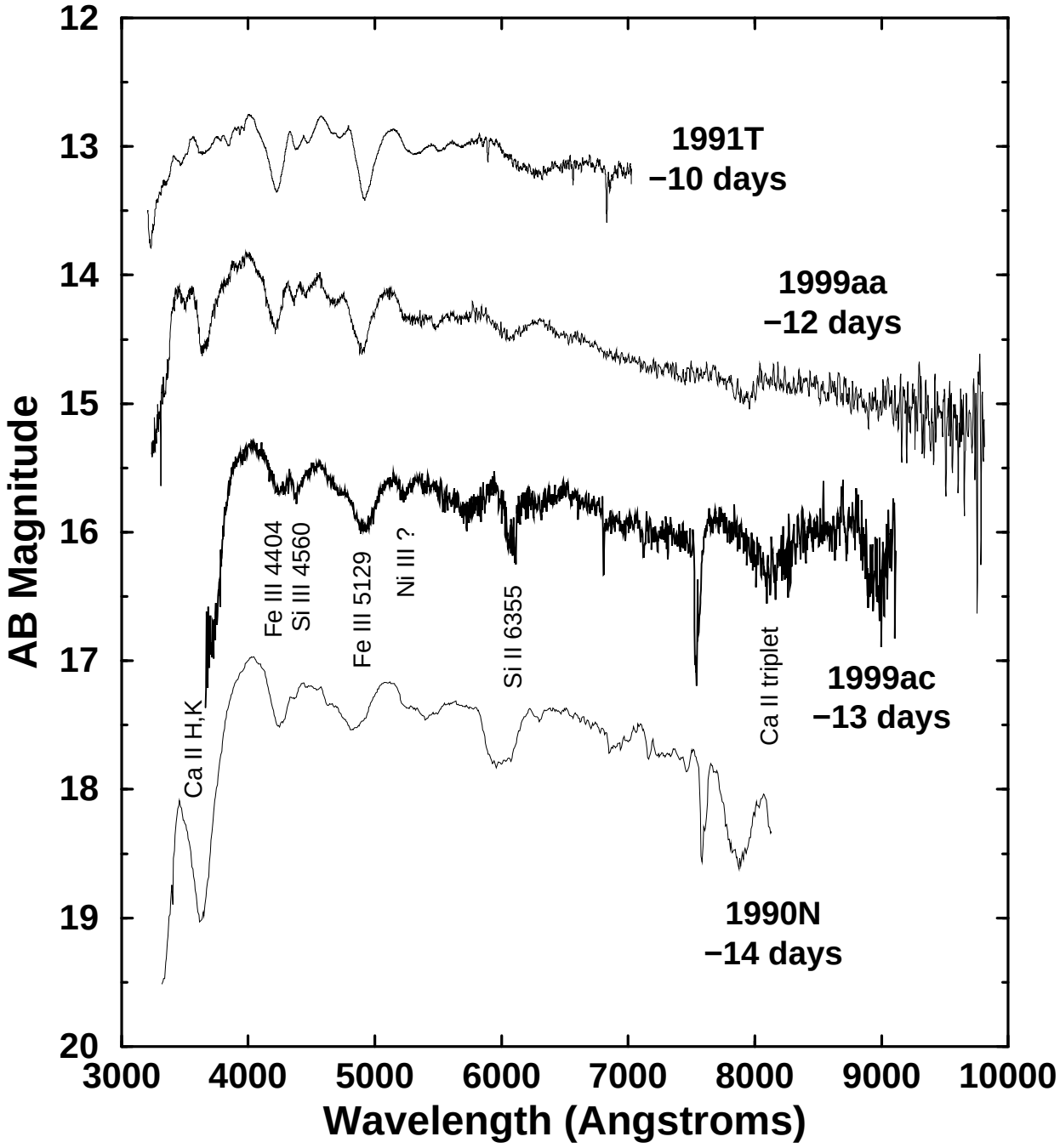

Phillips *et al.* Fig. 10

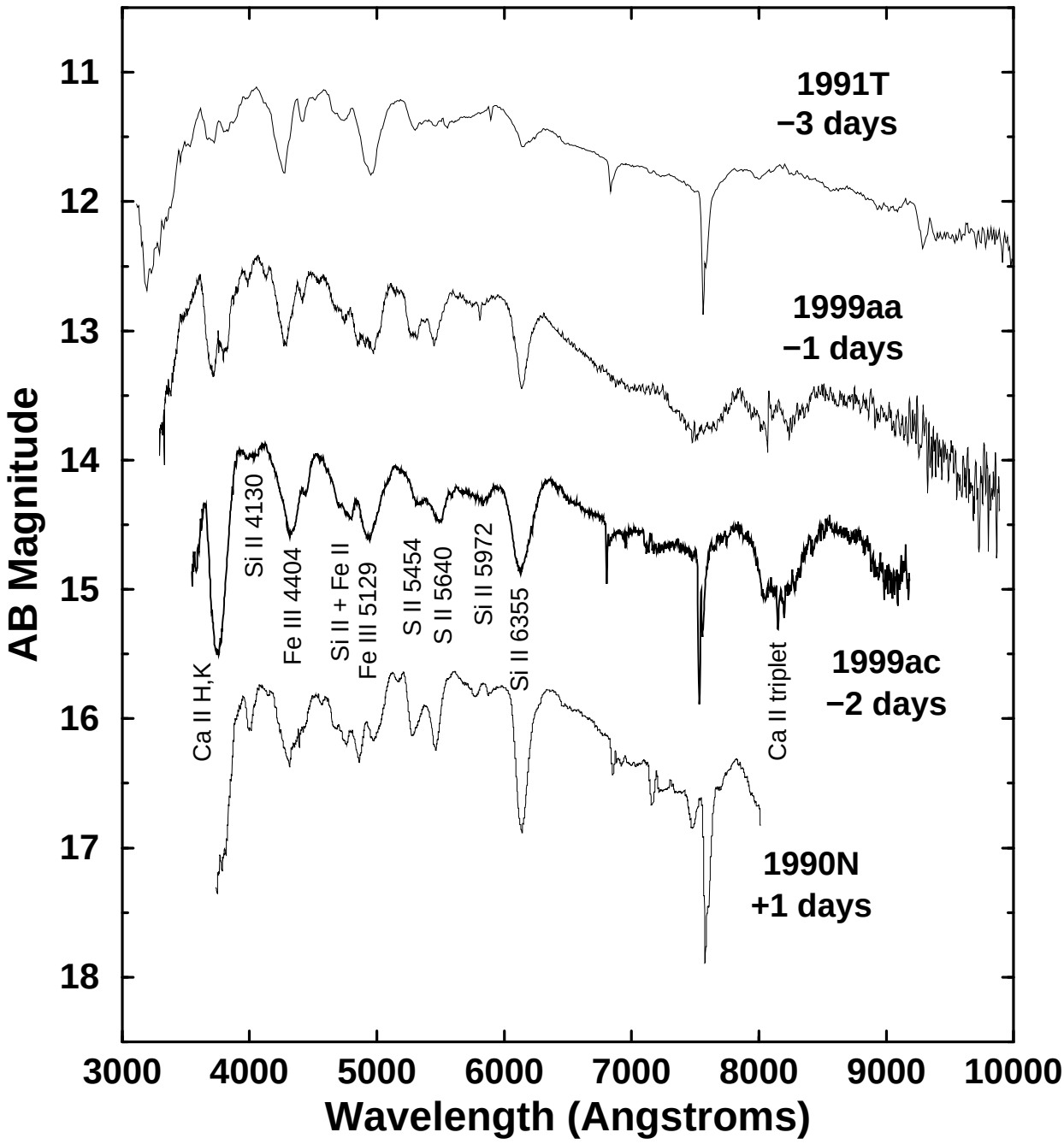

Phillips *et al.* Fig. 11

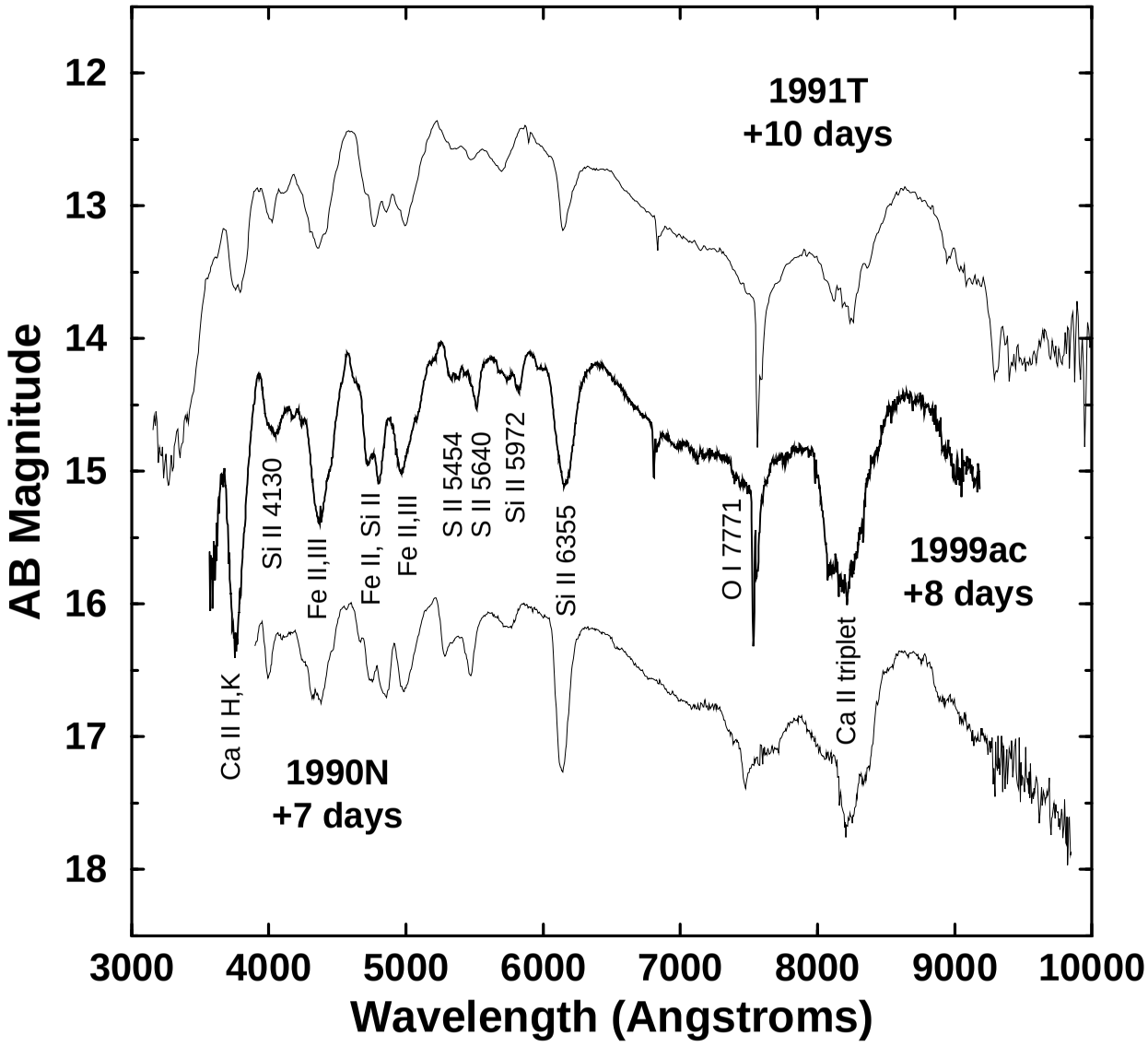

Phillips *et al.* Fig. 12

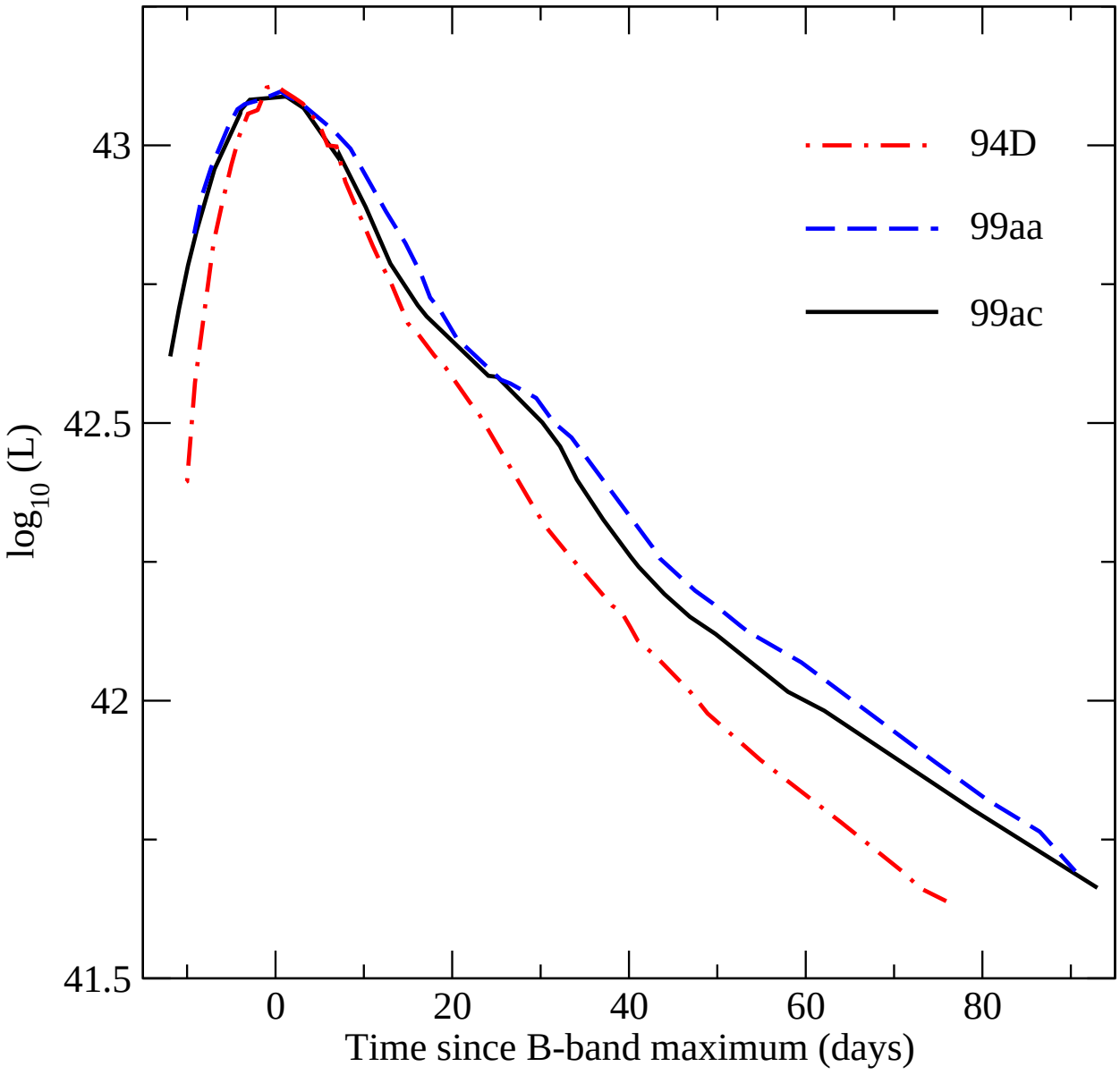

Phillips *et al.* Fig. 13

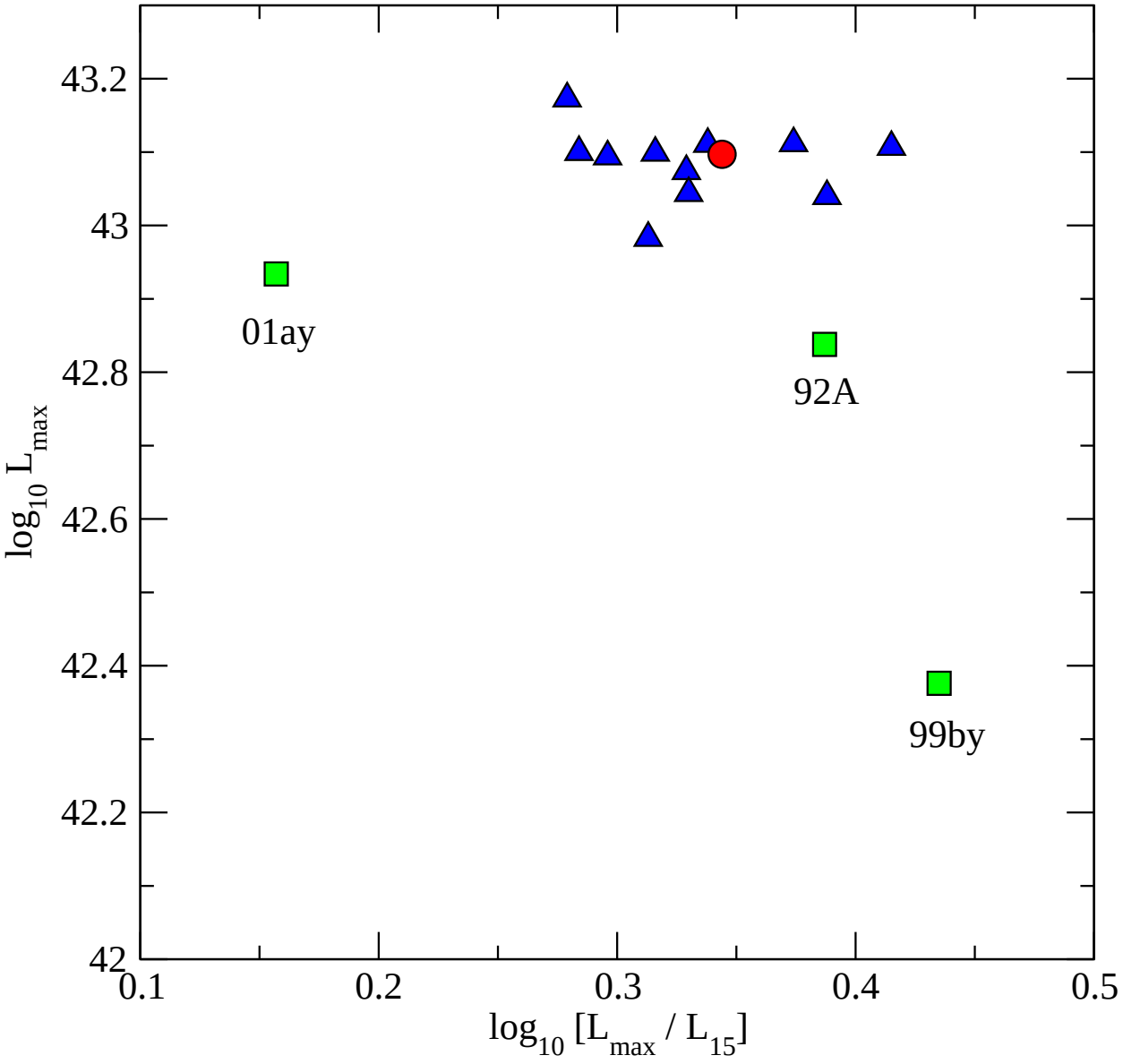

Phillips *et al.* Fig. 14